Degradation of Methyl Orange by Fenton Reaction using CuAl-layered double hydroxide/MgO_2 Composite Catalyst under Dark Condition

Setegn Geta Aragaw

A Thesis Submitted to

The Department of Materials Science and Engineering

School of Chemical, Mechanical and Materials Engineering

Presented in Partial Fulfillment of MSc Degree in Materials Science and Engineering

Office of Graduate Studies

Adama Science and Technology University

Adama

July, 2020

Degradation of Methyl Orange by Fenton Reaction using CuAl-LDH/MgO_2 Composite Catalyst under Dark Condition

Setegn Geta Aragaw

Advisor: Dr.Osman Ahmed

Co-advisor: Dr.Gebisa Bekele

A Thesis Submitted to

The department of Materials Science and Engineering

School of Chemical, Mechanical and Materials Engineering

Presented in Partial Fulfillment of MSc Degree in Materials Science and Engineering

Office of Graduate Studies

Adama Science and Technology University

Adama

July, 2020

Approval of Board of Examiners

We, the undersigned, members of the Board of Examiners of the final open defense by Setegn Geta have read and evaluated his thesis entitled "**Degradation of Methyl Orange by Fenton Reaction using CuAl-layered double hydroxide/MgO_2 Composite Catalyst under Dark Condition** " and examined the candidate. This is, therefore, to certify that the thesis has been accepted in partial fulfillment of the requirement of the Degree of Master's in Materials Science and Engineering.

Supervisor /Advisor	Signature	Date
Chairperson	Signature	Date
Internal Examiner	Signature	Date
External Examiner	Signature	Date

Declaration

I hereby declare that this MSc is my original work and has not been presented for a degree in any other university, and all sources of material used for this thesis have been duly acknowledged.

Name Signature Date

Setegn Geta

This MSc Thesis dissertation has been submitted for examination with my approval as thesis

Advisor Name Signature Date

Dr. Osman Ahmed

ACKNOWLEGMENTS

First and foremost, I would like to thank the almighty God for the good healthy that was crucial to finish this work. Wholeheartedly, I express my sincere thanks and profound gratitude to ASTU/SM-R/128/19 which lets me to take this opportunity. Furthermore, my deepest gratitude also goes to my advisor Dr. Osman Ahmed for his sound advice and encouragement. His maximum effort and motivational speech helps me to be strong and allows going forward**.**

Next, my thanks go to the entire department staff member who had been encouraging me side wisely. Among them my co advisor Dr. Gebisa Bekele who motivates me to acquire skills and perform the right thing even when the path seams tough, Dr.Dinsefa Mensur, Dr.Temesgen Debelo, Mr. Demeke Tesfaye, Mr. Andualem Mergia, Mr. Awoke Mheret, and others who helped me through their comments besides my classmates.

Profoundly, I would like to express my deepest gratitude to my department, Materials Science and Engineering. Without suffering a great challenge, we had finished here all the laboratory research works and some of the essential characterization techniques. It deals a great contribution not only for its members but also for other departments. Hope, it will persist its great dignity to build prolonged memory for Adama Science and Technology University at all.

At the end, I would like to forward my gratitude to all my parents who are always with me thereby providing encouragement and support all the year. Without them, today I will not be there.

Thank you

Setegn Geta

TABLE OF CONTENTS

ACKNOWLEGMENTS i
TABLE OF CONTENTS ii
LIST OF FIGURES iv
LIST OF TABLES v
NOMENCLATURE vi
ABSTRACT vii
1. INTRODUCTION 1
1.1. Statement of Problem 3
1.2. Scope of the Study 3
1.3. General Objective 3
1.4. Specific Objectives 3
2. LITERATURE REVIEW 4
2.1. Water Pollution 4
2.2. Wastewater Treatment` Techniques 4
2.2.1 Traditional techniques 5
2.2.2 Nanotechnology 5
2.3 Fenton Reaction 14
3. MATERIALS AND METHODS 18
3.1. Chemicals and Reagents 18
3.2. Apparatus and Instruments 18
3.3. Synthesis of CuAl-LDH Catalysts 18
3.4. Synthesis of MgO_2 18
3.4. Synthesis of CuAl-LDH/MgO_2 Composites 19
3.5. Characterization of the Catalyst 19
3.6. Catalytic Degradation 20
4. RESULTS AND DISCUSSIONS 21
4.1. XRD Result Analysis 21
4.2. SEM Analysis 22

4.3. FTIR Analysis 24
4.4. Catalytic Activity.....25
4.5. Effect of pH.....27
4.6. Trapping Experiments.....28
4.7. Kinetics of MO dye degradation 29
4.8. Re-usability Test.....30
4.9. Degradation Mechanism 31
5. CONCLUSION.....33
6. RECOMMENDATIONS.....34
7. REFERENCES 35

LIST OF FIGURES

Figure 2.1. p-n-p heterojunction in ZnO/CuO/$ZnFe_2O_4$ nanocomposite [40]. 8
Figure 2.2. LDH sheet [44].....9
Figure 2.3. Graphical abstract of CeO_2/MgAl- LDH composite [58].....11
Figure 2.4.Representation of methods of preparation and modification of LDH. https://ars.elscdn.com 12
Figure 4.1. XRD patterns of (a) MgO_2; (b) CuAl-LDH; (c) CuAl-LDH/MgO_2-7; (d) CuAl-LDH/MgO_2-10 and (e) CuAl-LDH/MgO_2-13 22
Figure 4.2. SEM images of (a) CuAl-LDH; (b) MgO_2; (c) CuAl-LDH/MgO_2-10; (d) EDX measurement of CuAl-LDH/MgO_2-10.....23
Figure 4.3. FTIR spectra of (a) CuAl-LDH; (b) CuAl-LDH/MgO_2-10 24
Figure 4.4. Absorbance versus wavelength patterns of (a) MgO_2; (b) CuAl-LDH; (C) CuAl-LDH/MgO_2-7; (d) CuAl-LDH/MgO_2-10 and (e) CuAl-LDH/MgO_2-13 26
Figure 4.5. Percentage removal versus time graph. 27
Figure 4.6. Effect of initial pH on MO degradation using CuAl-LDH/MgO_2-10 28
Figure 4.7. Radical quenching effect on MO degradation using CuAl-LDH/MgO_2-10.....29
Figure 4.8. (a) degradation kinetics of MO by different catalysts and (b) bar diagram plot of rate constant values for different catalysts 30
Figure 4.9. (a) Re-usability and (b) XRD of CuAl-LDH/MgO_2 -10 before and after cyclic test. .31
Figure 4.10. Schematic diagram of catalysis to degrade MO.....32

LIST OF TABLES

Table 2.1. Summary of LDH based studies.....12
Table 2.2. Comparison of active oxygen content and purity of different oxidants 16
Table 4.1. First order rate constant for MO.....30

NOMENCLATURE

LDH	Layered double hydroxide
•OH	Hydroxyl radical
ROS	Reactive oxygen species
AOP	Advanced oxidation process
MMO	Mixed metal oxides
K_1	Rate constant for Pseudo-first kinetics (min^{-1})
C_o	Initial concentration (mg/L)
C_t	Concentration at a given time‘t’ (mg/L)
D	Crystalline size (nm)
CB	Conduction band
VB	Valance band
R	Regression coefficient
MO	Methyl orange

ABSTRACT

Water pollution due to organic dyes has been a global issue. Because dyes own stability and able to soluble in aqueous media. As a result, dyes stay for prolonged time while water gets polluted with such kinds of effluents. In order to minimize the amount of effluent in the polluted water, enormous methods have been proposed. In typical, Fenton reaction has been used. However, the sludge formation under iron based Fenton, dependent on light irradiation and the need of acidic media limits its application. In this report, CuAl-layered double hydroxide/MgO_2 composite was synthesized through in-situ growth of magnesium peroxide on the LDH sheet. Profoundly, it has performed well over wide pH range as well under dark environment which in turn minimized the requirement of light irradiation. In this case unlike the conventional Fenton process, there was no difficulty in transporting and handling of peroxide since generating H_2O_2 through in-situ way. As-synthesized powders were characterized and performances were evaluated for methyl orange (MO) dye degradation at room temperature. X-ray powder diffractometer (XRD), scanning electron microscope (SEM), and Fourier-transform infrared spectroscopy (FTIR) were used for characterization. The catalytic activity of CuAl-LDH, MgO_2, CuAl-LDH/ MgO_2 -7, CuAl-LDH/ MgO_2 -10 and CuAl-LDH/ MgO_2 -13 were investigated for the degradation of methyl orange (MO) under dark. Among them, CuAl-LDH/ MgO_2 -10 shows excellent Fenton like reaction under neutral condition at which 97% of MO was degraded with in 100min. While 98% of MO removal was achieved at acidic pH within 60 min. The higher degradation efficiency by this particular composite is attributed to the presence of copper along with the generated hydrogen peroxide to run Fenton process. Trapping experiment values also confirmed that both copper and hydroxyl radical were an active species for the degradation of MO. Moreover, the catalyst can also be able to use for several cycles with a minimum loss of activity. In general, the result of this study suggests that CuAl-LDHMgO_2-10 composite is an option for the conventional Fenton based degradation of MO under dark environment.

Key words**: **Fenton reaction; layered double hydroxide; metal peroxide.

1. INTRODUCTION

Now a days, organic pollutants such as phenols, pesticides, dyes, and other pollutants are a great concern to the environment [1]. Since the development of industries takes several chemicals as input, effects related to effluents gets worse. It is known that the human life standard is directly affected by the quality of air, water, and soil. Particularly, chemicals released from industries and population growths are also the main causes for water pollution and have led an adverse issue on healthy life [2]. Therefore, the decontamination of polluted water resources is now the main concern for the researchers in the globe. Although several usual water treatment methods such as filtration [3], sedimentation [4], and distillation [5] were pointed out, those methods mostly known by limitations for complete removal of pollutants besides consuming time. Other methods such as adsorption, catalytic oxidation, and photocatalytic degradation [6] have been also used for wastewater treatment. It is known that the adsorption and chemical catalytic oxidation have been the basic approaches for pollutant removal [7]. Because such methods allow to remove pollutants unselectively than the traditional counterparts do. It is also reported that the photocatalysis is effective and efficient method for treatment of wastewater [8]. It involves the production of hydroxyl radical •OH as well other active oxygen species in the photocatalysis, electrochemical oxidation, photo-Fenton, Fenton and Fenton-like processes. Those methods are known by utilizing highly reactive oxidizing agent like hydroxyl radical [9]. The reactive oxygen species can unselectively decolorize wastewater through converting toxic pollutants to non-toxic species like CO_2 and H_2O [10]. For this purpose metal oxide catalysts can be used due to economical, efficiency and stability.

Metal oxides such as TiO_2, and ZnO are important class of materials for wastewater treatment. However, they have their own limitations such as high recombination rate due to large band gap, unable to be re-used, and high agglomeration and uncontrolled crystal size [8]. Therefore, the metal oxide nanoparticles should be grown onto supporting materials to minimize agglomeration effects for improving catalytic activities. In this perspective, layered materials, and clays like bentonite has been used as a support for metal oxides and the supporting materials can help to immobilize metal oxides and reduces agglomeration thereby providing a site for growth [11]. In addition to bentonite, the layered double hydroxide (LDHs) also named as synthetic anionic clay-like layered materials have been studied to treat pollutants through both

adsorption and degradation process owing to their layered and special memorial property than the usual known metal oxides [12]. Owing to their unique memory effect properties, LDHs are stable [13]. Moreover, LDHs can also provide a good dispersion for metal oxides upon reducing agglomeration effect [14].

It is reported that the Fenton-like advanced oxidation process is a promising technology for the prompting of strong oxidants even at dark environment [15]. Particularly, the iron has advantages due to plentiful abundance, low cost, adaptable to the environment, and low-poisonous. However, iron based Fenton reactions always requires extremely acidic environment, difficulty in hydrogen peroxide transportation, and leads to lower life time during oxidation. Moreover, the traditional Fenton-related operation is also limited to an acidic medium with pH range of less than of 4.0. Thus, many researchers have been engaged in the modification so as to overcome the challenges present in conventional Fenton processes. Among the findings, using non-ferrous based catalysts, and *in-situ* generation of peroxide have been reported and showed an intensified performance [16, 17]. Such findings not only broaden Fenton like activity to a wider pH range but also minimize the loss of catalyst through precipitation. Particularly, the Cu-based catalysts in Fenton-like reactions can provide great potential in Fenton reactions under neutral pH which is not common in iron based Fenton [18]. This tells that the possibility of copper based Fenton reaction to work over wide pH range. The reactive oxygen families are also formed after the reaction between Cu ions and H_2O_2 and it act as an active species for pollutant degradation. Thus, it is better to find out non-iron based Fenton systems which can able to work over a broad pH range. Among the various options, forming heterojunction is greatly recommended to fix drawbacks presented in metal oxides.

In this work, a composite of CuAl-LDH and magnesium peroxide catalyst is reported for methyl orange dye degradation under dark condition. As-synthesized CuAl-LDH/MgO_2 composite provides a synergistic benefit from each individual for optimum performance upon degrading methyl orange (MO). CuAl-LDH maintains a good stability for the growth of MgO_2 particles.

1.1. Statement of Problem

In most extent, treatment of wastewater effluents has been a challenging issue. The sludge formation in iron based Fenton like reactions is also a common challenge. As a result, non-iron based Fenton reactions have got a greater appreciation owing to working over a broad pH range besides lowering sludge formation. However, unstable nature and difficulty of storing the liquid H_2O_2 leads lower efficiency in Fenton reaction system to generate oxygen radicals. For example, CuAl-LDH was synthesized but owns lower recyclability due to unstable nature and in adequate transportation of H_2O_2 towards the active site of catalyst. Thus, it is better to use other potential oxidants like metal peroxides which can able to generate H_2O_2 through in-situ way in aqueous media. Hence, by realizing the synergistic benefits of forming a composite, coupling metal peroxides with LDHs can lead easier transportation of an oxidant, broader light response range and sufficient hindering of charge recombination.

1.2. Scope of the Study

In this work, CuAl-layered double hydroxide, magnesium peroxide (MgO_2), and a composite of them (CuAl-LDH/MgO_2) were synthesized through co-precipitation route. After characterization, performances of as-synthesized samples were evaluated in the absence of light irradiation for methyl orange (MO) dye degradation followed by selection of the optimal catalyst. Later on, effect of pH, kinetic study, trapping experiments, and stability test were studied.

1.3. General Objective

To synthesis and characterize CuAl-layered double hydroxides/MgO_2 based nanocomposite for treating methyl orange.

1.4. Specific Objectives

- Synthesizing CuAl-layered double hydroxide (CuAl-LDH) and MgO_2;
- in-situ growth of magnesium peroxides on the CuAl-LDH sheet in a solution;
- Optimizing the composite by using different mass concentration;
- Characterization of each individual results for confirmation;
- Apply CuAl-LDH, MgO_2 and CuAl-LDH/MgO_2 methyl orange dye degradation.

2. LITERATURE REVIEW

2.1. Water Pollution

There is no any doubt at which water is important to sustain the continuity of life. But globally there is a problem of water contamination due to the presence of organic and inorganic impurities. Among the causes for water pollution are industrial effluents, detergents, bacteria, Plant debris, and unsafe sewage disposals are commonly happened [19]. In addition to effects on aquatic life, the pollution of water leads various effects on the atmosphere, social relation, growth production level etc. About 1.7 million persons passed away every year due to water contamination as word healthy organization demonstrated [20]. Thus, the availability of pure water is a global issue that needs great consideration.

On account of wastewater composition and discharge volume of all industrial sectors, textile industry is the most polluting [21]. Various adapted methods like filtration, evaporation, and distillation were utilized to treat water as pure as possible. Apparently, nanomaterials are surprisingly used for adsorption, and catalysis so as to make water more pure than traditional counterparts. Although complete decolorization is challenging due to dyes complex structure and stability, advanced oxidation process is crucial to enhance atmospheric air quality and to decompose pollutants. Moreover, advanced oxidation process provides benefits like excellent efficiency, fair cost, sustainable activity than the usual methods, and will lead complete degradation. Despite such benefits, the toxicity and reusability of catalysts are still the limiting factors upon application. To solve reusability issue, scientists have synthesized magnetic catalysts so as to remove using external magnets.

2.2. Wastewater Treatment`Techniques

Since water is very important for every walk of life, treating water was put in the eyes of researchers' world widely. They have tried to bring out new technologies with enough efficiency in combined with fair cost [22].

2.2.1. Traditional techniques

The normal reception techniques such as sedimentation, coagulation, decantation, and osmosis are inefficient to remove pollutants. For instance, coagulation is done by adding iron and aluminum salts to the water [23]. It can only neutralize negatively charged species. In other word, it is not sufficient to cure the wasted water. Therefore, advanced treatment is needed for sufficient treatment.

2.2.2. Nanotechnology

Nanoparticles have gained a promising option to overcome issues associated with water pollution. More importantly, nanomaterials brought unique properties owing to their higher surface area, small size or high reactivity and well dispersability [24]. The higher specific surface area and magnetic property allows them to adsorb excellently. Wasted water may contain heavy metal such as Hg, Pb, Mo, besides organic and inorganic pollutants which all needs to be early treated before worst effect happened. Adsorption is preferable due to effectiveness for a range of pollutant, ease operation, flexibility, and minimum cost [25]. The Semiconductor metal oxides, heterojunctions, and LDHs were applicable to make discharged water safe. In some instance, metal oxides face a problem upon controlling their size in the desired range. It is common that as sizes gets small and small, reactivity also enhanced. However, it needs other supporting materials to minimize aggregation effect to insure the cyclic usage. Although the existence of drawbacks is common, nanomaterials have high potential for water purification along with a very effective approach [26].

2.2.2.1. Metal Oxides (MOs)

Various metal oxide semiconductors like WO_3, TiO_2, SnO_2, and NbO_2 had been used for water treatment under UV and visible light irradiation [27]. Despite the large band gap of metal oxides like ZnO (3.2 eV) and MgO (7.83eV), both have got greatest consideration owing to low cost, low toxicity, and possibility of mass production [28]. Magnesium oxide has its own benefits like nontoxic, low cost and environmental friendly that was utilized in antibacterial activity as well as heavy metal adsorbents [29]. Aqueous form of MgO forms magnesium hydroxide which then dissociates into OH^- that leads for adsorption of heavy metals.

Nanomaterials are also difficult to separate from a solution due to their small size. Unsteady state also leads to aggregation outcome. One approach to overcome this problem is work for further improvement on the synthesis process. Several reports proved that through doping and co doping, it is possible to easier recoverability, and improve performance [30]. Nickel doped magnesium oxide through green synthesis route applying on the local accessible plant named as Synadenium grantii was reported by Chen J *et al*.[31]. Nickel doped magnesium oxide showed better methylene blue degradation than pure MgO. Moreover, crystalline size was reduced from 29 nm to 20 nm upon using green mediated route. As a recent report stated that, the antibacterial activity of silver doped MgO was better than both pure MgO and Ag [32]. Silver enhances the production of ROS thereby promoting electron transfer.

Similarly, the large band gap of zinc oxide had been modified by doping with cadmium for phenol degradation [33]. Doping is done to extend absorption band towards the visible region. Co-catalyst has been also used to hinder recombination through providing additional active site, interfacial charge transfer and acting as electron sink. Cu^{2+} was utilized as a co-catalyst to make zinc oxide active under visible light radiation. As stated in the report on modification of zinc oxide, Cu^{2+}- ZnO showed an enhanced antibacterial activity than pure ZnO and pure TiO_2 [34]. In addition to cation doping, anion doping into wide band gap semiconductors can be used for the reduction of energy gap. Sulphur containing zinc oxide nanoparticle ($ZnO_{1-x}S_x$) was synthesized using ZnO (3.37ev) and ZnS (3.5 eV) as a staring material [35]. As doping is limited by the maximum dopability of the material, a new technique was suggested to reduce band gap is through forming a composite of ZnO and ZnS which resulted 2.07eV [36]. However, pristine metal oxides mostly encountered a challenge of sufficient charge transportation besides unable to suppress recombination effect. Therefore, it is better to combine metal oxides with other materials.

In addition to doping, a junction between metal oxides has been advisable to extend the light response range of the individual metal oxides. Limitation of most photocatalysts is basically circled on the insufficient solar light conversion efficiency owing to wide band gap value and a consequence of low cycle life [37]. Many works have been done to form a junction between materials. Reda *et al*.[38] stated for RhB dye photo degradation using Co_3O_4-ZnO p-n heterojunction which effectively reduces recombination through forming internal electric field at

the junction interface. Because electric field is formed at the depletion region once charge carriers drift in between Co_3O_4 and ZnO. They confirmed that photocatalytic activity of Co_3O_4-ZnO was five times enhanced than done by ZnO. It is due to higher surface area and inhibiting recombination obtained by the composite.

Ternary Ag/ZnO/$ZnFe_2O_4$ also shows better photocatalytic activity than binary counterpart of ZnO/$ZnFe_2O_4$ towards organic dye degradation [39]. The study had showed that recombination of photogenerated electron-hole pairs can be inhibited by the combination of Ag, ZnO and $ZnFe_2O_4$ through forming type II-band alignment and schottky barrier. Although $ZnFe_2O_4$ can absorb visible light due to lower band gap value (1.9 eV), photo generated electron hole pairs recombine rapidly. Consequently, ZnF_2O_4 shows poor photocatalytic activity. Once ZnO and $ZnFe_2O_4$ combined, they can form ZnO/$ZnFe_2O_4$ composite. Moreover, both the conduction band and the valance band value of $ZnFe_2O_4$ are less negative than ZnO, it can form type-II band alignment. Therefore, recombination can be suppressed sufficiently as electrons move to the CB of ZnO while holes are remain in the VB of $ZnFe_2O_4$. On account of schottky barrier formation, some of photogenerated electrons transferred from CB of ZnO to the silver surface. Another ternary nano composite material, ZnO/CuO/$ZnFe_2O_4$, was synthesized by calcining the co-precipitation of $Zn(NO_3)_2$, $Cu(NO_3)_2$ and $Fe(NO_3)_3$ solutions [40]. It was applied for MO removal. Here, the presence of narrower band gap CuO facilitates the near-infrared region (NIR) photo Fenton like activity of ZnO. Initially, ZnO can only absorb in the UV region while incorporating $ZnFe_2O_4$ it just extends the absorption range to the visible region. Further introducing CuO, extends absorption to NIR region. The above justifications are already simplified as shown in Figure 2.1 below.

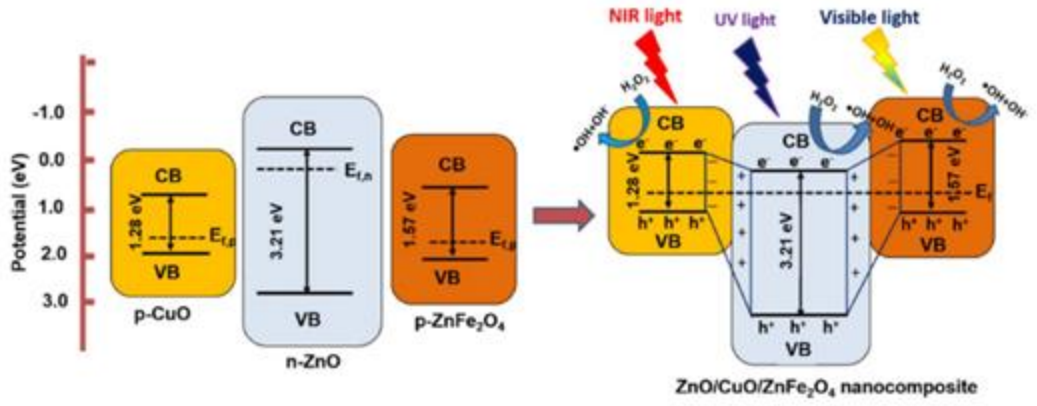

Figure 2.1. p-n-p heterojunction in $ZnO/CuO/ZnFe_2O_4$ nanocomposite [40].

2.2.2.2. Layered Double Hydroxides (LDHs)

Beside metal oxides, layered double hydroxides are also effective in treating pollutants through both adsorption and degradation process owing to their stability and owned a special property [12]. The higher accessible surface area enables them to adsorb toxic substances from wastewater. LDHs have a general formula $[M^{+2}_{1-x}M^{3+}_{x}(OH)_2]^{+x}$ $(A_{x/n})^{n-}.mH_2O$, also called hydrotalcite clay since they are derived from the natural available mineral, $Mg_6Al_2(OH)_{16}CO_3.4H_2O$. Where M^{+2} and M^{3+} are cations valance number , x is molar fraction of metal ions and A^{n-} is inter layer anions like CO_3^{2-}, NO_3^-, and Cl^- which are charge balancing anions [41]. Because of possessing some of clays properties, LDHs are also called anionic clay. Swelling in water, wide composition due to isomorphically substitution of various metal cations, reactive species, and colloidal property all makes LDHs as clay like [42]. LDHs itself can perform as catalyst, as precursor for other catalysts and as catalyst support for various applications [43]. LDHs own several unique properties such as, a special memory effect, good stability, cheap, and easy to prepare. Figure 2.2 as shown below displays a general structural feature of LDHs. It shows a layered arrangement containing anions on its interior part. The layered structure is preserved by an existed water and hydroxyl anions on the inter layer.

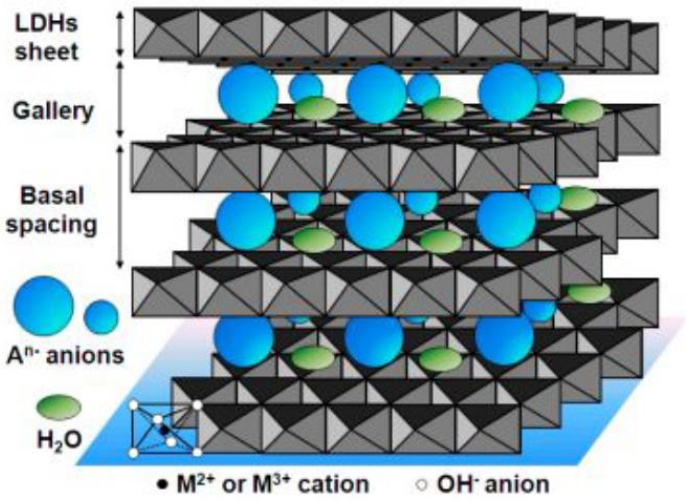

Figure 2.2. LDH sheet [44]

There are many reports on LDH catalysts for different applications [45-48]. Here are some of LDH-based works reported for different applications. Synthesis of biodiesel using MgAl-LDHs was reported by Hsu *et al.*[49]. Jia *et al.*[50] also summarized the amine-functionalized MgAl LDH nanosheets for Knoevenagel condensation. Another highly crystalline CuAl-LDH was reported by Li *et al.* for methyl orange degradation through Fenton reaction [51]. The trend for MO degradation was pointed out as CuAl-LDH > MgAlCu-LDH > MgAl-LDH. These sequences tell that the degradation of MO is dependent on the content of copper ion. But their result showed lower re-usability because of hindering hydrogen peroxide in making contact with the active sites in combined with adsorption of pollutant intermediates on the surface. Having sheet like morphology, Cu/Zn/Al nanocatalysts derived from LDH/MOF composites was also done for CO_2 hydrogenation to methanol as reported by Zhao *et al.*[46]. NiFe-layered double hydroxide/ graphene oxide was also reported by Cao *et al.* [52]. It was applied for oxygen reduction. Furthermore, Zhao *et al.*[53] also used Co/Ni LDHs for dye wastewater treatment. NiAlCe–LDH also pointed out for organic dye wastewater degradation by Tao *et al.* [54]. However, the efficiencies of LDHs alone are lower under visible light irradiation. Hence, the low energy conversion efficiency in LDH can be suppressed by dispersing photoactive species in the LDH. Due to this reason, it is important to make composite with other semiconductor materials or metal nanoparticles for effective utilization of sunlight energy.

2.2.2.3. LDH-MO junctions

A composite of LDH and metal oxides were used for different applications. Primarily, such blending helps to extend the light absorption range as well as suppressing recombination of photogenerated carriers. Recently, a novel Ni–Fe LDH/ZnO composite was synthesized for the degradation of Rhodamine B.dye under light [55]. On the other work, in addition to dye degradation, Ni–Fe LDH/ZnO nanostructures was proved for water splitting by Mustafa *et al.* [56]. It was found that the dissolution of ZnO under light irradiation has been reduced through combining with LDH than shown in pristine ZnO. Seftel *et al.*[14] also synthesized a composite of CeO_2 nanoparticles with ZnTi-LDHs for phenol degradation. Nanoparticles of CeO_2 were grown through in-situ way on to the reconstructed calcined ZnTi LDH surface at room temperature. The composite material showed better thermal stability than pristine CeO_2. Because very high temperature is needed to remove sulfate ions in the interlayer region. Zheng *et al.* also synthesized NiAl-LDH/MnO_2 and NiFe-LDH/MnO_2 composites for high-performance asymmetric supercapacitors [57]. It has been synthesized by loading of MnO_2 on LDH nanosheets with the aid of redox reaction. In the same way, CeO_2 has been used to extend absorption towards visible light (Vl) region. Despite various CeO_2 used for Vl-active photocatalysis, CeO_2 still needs a support for better stability and suppressing charge recombination. Considering this idea, Nayak *et al*. showed a visible light induced CeO_2/MgAl-LDH for water reduction as shown schematically in Figure 2.3 [58]. Optimization had been done through varying the dose of $Ce(NO_3)_3.6H_2O$. Specifically they found that 5 wt% CeO_2 exhibits higher photo catalytic activity. At 5 wt% CeO_2, CeO_2 nanorods size is narrower thus allows to homogeneously distribute and leads high surface area. CeO_2 also plays a role by reducing diffusion path for charge carriers and makes easy transfer of surface charge to the surface of MgAl-LDH. Excessive CeO_2 may not bring enhanced activity due to shielding effect, agglomeration of CeO_2 nanorods and reduction of interfacial area. Consequently active sites wrapped in response to excessive CeO_2 so that H_2 production level gets minimum.

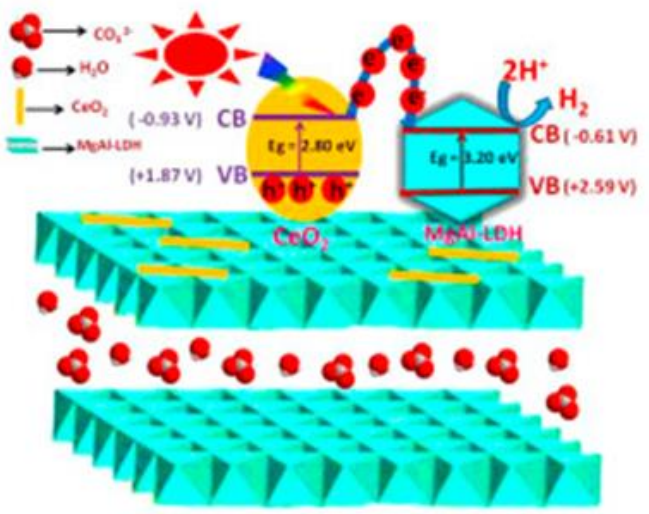

Figure 2.3. Graphical abstract of CeO_2/MgAl- LDH composite [58]

With a similar manner, the light response of TiO_2 was improved by combining TiO_2 with MgAl LDH as reported by Lu *et al.*[59]. The LDH functioned as a support to well disperse TiO_2 nanoparticles. Another LDH supported metal oxide, ZnO-MgAl LDH composite was also reported by Zhi *et al.*[60]. The composite material showed good dispersion of ZnO nanoparticles on the LDH surface without aggregation so that better accessible area and adsorption capacity maintained.

Furthermore, many research works have been done on exchanging foreign anionic species in the interlayer of LDH. Using this method, MgAl-LDH intercalated with EDTA which acts as a chelator was synthesized to take up heavy metal ions like Cu^{2+}, Cd^{2+}, and Pb^{2+} from water [61]. But citrate, tartrate, and malate intercalated LDH are more suitable than EDTA-LDH. It is due to the availability and huge commercial usage. Carboxylate ions such as citrate, oxalate, tartrate, and malate were also intercalated with MgAl-LDH [62]. Principally they aimed to produce carboxylic acid intercalated LDH through reconstruction method from calcined LDH (LDO) other than using the usual co-precipitation method. But, this new way of synthesizing route helps to reduce the presence of other un-wanted anions like chloride, nitrate, and carbonates besides able to work under free of nitrogen-atmosphere. Also, an ionic surfactant named Sodium dodecylsulfonate (SDS) is intercalated into Mg-Fe-LDH and acts as a structure directing agent through changing the inter layer distance besides modifying cluster state of crystals [63]. Figure 2.4 shows that LDHs can act as a precursor for synthesizing metal oxides as well owns a memory

effect behavior. In other word, if necessary, it can maintain its originality upon reconstructing metal oxides in a solution.

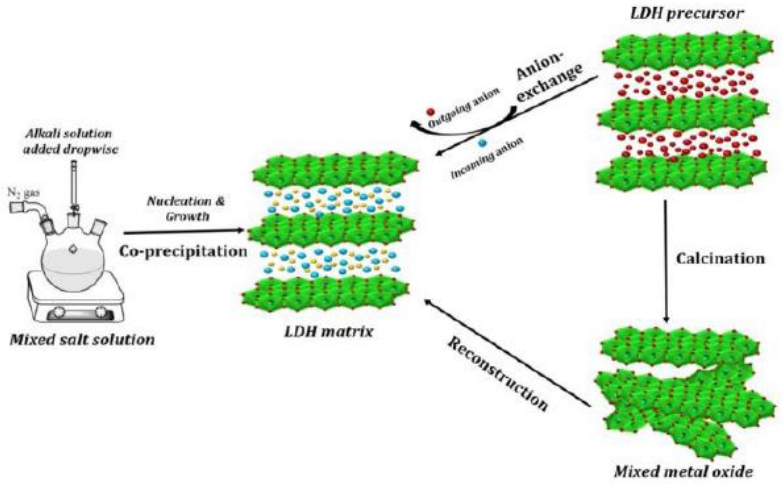

Figure 2.4.Representation of methods of preparation and modification of LDH. https://ars.elscdn.com

The following tabulated works are LDH based reports for different activity with improved result than the pristine materials brought.

Table 2.1. Summary of LDH based studies

LDHs	Working Mechanism	Activity	Pollutant type or chemicals	Ref.
CeO_2-ZnTi LDH	Photodegradation	90% of phenol is completely removed	Phenol	[14]
ZnO-MgAl LDH	Adsorption	BET surface area of MMO (257 m^2/g) is much larger than LDH (87 m^2/g)	Acid red G	[60]
Cu_2O/ZnAl-LDO	Photodegradation	90.18% under visible light	Methyl orange (MO)	[64]

CeO_2-MgAl-LDH	Photodegradtion	Degrade~96% of 100ppm of 4-cp in 5hr.	Phenol	[65]
CeO_2-MgAl-LDH	Oxidation	H_2 evolution rate is 990w/c is 1.98 times than pure CeO_2	Water splitting	[58]
WO_3/Fe_2O_3/NiFe-LDH	Oxidation	Photocurrent density of 3mAcm^{-2}, which are 5 times and 7 times of WO_3 and α-Fe_2O_3.	Water splitting	[66]
ZnS-ZnO/ZnAl-LDH	Photocatalysis	H_2 production of 1599 μmolh^{-1}g^{-1}	Water splitting	[67]
WO_{3-X}/Ag/ZnCr LDH	Visible Light-Induced Photocatalyst	H_2 evolution (29375 μmol g^{-1} h^{-1}) & TC removal (92% in 90 min)	Tetracycline degradation and H_2 Evolution	[68]
Ag_3PO_4-ZnAl-LDO	Photodegradation	49.3 times as high as that of pure Ag_3PO_4	Tetracycline	[69]
Nb_2O_5-ZnAl-LDH	Photodegradation	85% degrade under visible light	Congo red	[70]
CuAl-LDH	Photodegradation	99.1% in 10 min	Methyl orange (MO)	[51]
Starch –NiFe-LDH	Adsorption	Maximum removal of 99 and 90%	Anionic methyl orange	[71]
CoAl-LDH@$BiVO_4$	Photoelectro-chemical	2-fold enhancement in the oxidation efficiency and IPCE value	Water oxidation	[72]
TiO_2/GR/NiFe-LDH	Photo-electrochemical	Photo-conversion efficiency (0.58% at 0.13 V) and	water splitting	[73]

		photocurrent density(1.74 mA cm^{-2} at 0.6 V)		
LDH-based CoO–$NiFe_2O_4$	Fenton-like Adsorption and catalysis coexist	87–97% decolorization of Eriochrome black T dye (EB) within 120 min	Adsorption and catalysis coexist	[74]

2.3 Fenton Reaction

Relative to the other AOPs, Fenton process is easy to run, does not need other energy, and able to degrade many pollutants non-selectively. Fenton process is based on iron and its compounds as a catalyst. During Fenton process, hydrogen peroxide just reacts with iron to bring out reactive species. Although it is crucial, the liquid nature of hydrogen peroxide is unstable, and will easily decompose [75]. In spite of the easier working mechanism, the classical Fenton process always works on acidic range. It cannot work at a pH range out of acidic media. As the pH gets above 4, iron sludge forms which eliminates the cycle of reactive oxygen species generation. Generally, an optimal pH range is required. In some instance, low pH does not always lead enhanced pollutant degradation. Owing to the acidic environment, part of catalysts will leach out, unable to recycle, and need of more filtration before discharge the solution. In addition to losing the active species, the sludge formation at high pH will also lead secondary waste on the environment [76]. All those drawbacks put a black hole on the most unique benefits obtained by Fenton process. Therefore, optimization is required for overcoming the drawbacks of the conventional Fenton process.

Heterogeneous Fenton process is one of the optimization processes for the conventional Fenton process. The loss of iron species has been resolved by using heterogeneous Fenton process. In doing so iron species immobilized on the supports like clay [77], and graphene [78]. Such supporters prevent iron species from immersing in the solution as it gives a site for long term persistence [79]. Realizing the synergistic benefits, iron-copper bimetallic was synthesized to enhance catalysis at neutral environment [80]. In addition to the higher rate of cycling Cu^{+}/Cu^{2+} than Fe^{2+}/Fe^{3+}, copper can react with H_2O_2 and able to work on broad pH range .

Heterogeneous electro-Fenton process has better stability, large pH range workability and reusability than conventional Fenton process [81].

Unlike Heterogeneous Fenton process, the other Fenton optimizations require extra energy. Photo-Fenton is one of the energy based optimization method which uses ultraviolet or visible light to facilitate the reduction of Fe^{3+} to Fe^{2+}. Under photo Fenton reaction, H_2O_2 is decomposed to hydroxyl radical with the aid of Fe ions. Besides maintain the cycle of iron species, the light will lead to direct decomposition of H_2O_2 into hydroxyl radical [82]. Maezono *et al*. reported that Photo Fenton is effective for discoloration of Orange II [83]. They had proved that UV light caused not only the generation of •OH radicals but also facilitates the iron cycle.

The other optimization for conventional Fenton process is electro-Fenton process. The name electro-Fenton stands from the combination of conventional Fenton process with electrochemistry. The basic target in this method is to reduce handling, transportation and storage difficulty of H_2O_2 as well as maintain the cycle of iron species. During the process, H_2O_2 is in situ way generated through the reduction of O_2 on the cathode [84]. Additionally iron sludge production is reduced and the oxidized iron also reduced to Fe^{2+}on the cathode. Even though the way electro-Fenton process works is interesting, the low yield of H_2O_2, low current density and low conductivity are the common drawbacks. As reported by Ganiyu *et al*. electro-Fenton process works over a broad pH range [85]. They proved that 66% of organic pollutants were removed with in the pH range between 2 and 7.1. Generally, not only optimal pH range but also the concentration of hydrogen peroxide concentration should be limited. Under Fenton process, it is common that removal efficiency increases with the increasing of H_2O_2 concentration. But, excess H_2O_2 will reduce the available •OH thereby scavenging effect [86]. All the above listed optimizations haven't brought cost beneficial. Therefore, it is preferable to find out other alternative materials which can overcome these problems. In other words, instead of externally add hydrogen peroxide, focusing on in-situ way of generating H_2O_2 is advisable. Previously, the difficulty of transportation and storing the liquid hydrogen peroxide was common. The direct synthesis of H_2O_2 using precious metals like gold, silver, and platinum to catalyze the reaction between H_2 and O_2 were adapted. But, this approach has limitations like cost due to precious metals, and the minimum solubility of O_2 and H_2 in water [87].

As a result, this time, in-situ generation of H_2O_2 has attracted much attention. For instance, Yang *et al.* observed magnesium–carbon nanotube composites for the in situ generation of H_2O_2 [88]. Recently, CNTs-Fe-Cu composite was also produced by a liquid phase reduction method and able to work even at neutral condition besides generating H_2O_2 for the degradation of sulfamerazine [89]. Similarly, Zn-Fe-CNTs was synthesized for sulfamethoxazole degradation [90]. But, it results low productivity of H_2O_2 than copper based Fenton performs. As it can able to perform at neutral condition, there is no need of treatment for the discharged solution at the end of reaction. The in-situ generated H_2O_2 immediately converted into the reactive oxygen species radicals by CNTs-Fe-Cu. This leads not only the reduction of risks upon transportations of H_2O_2 but also accelerated the efficient utilization H_2O_2.

Profoundly, metal peroxides like CaO_2, NaO_2, and MgO_2 have been also considered as an alternative source of hydrogen peroxide and confirmed to be a technically feasible to run Fenton process. Recently, MgO_2 were used as a best alternative oxidant [91]. Although the decomposition of H_2O_2 is catalyzed by Fe^{3+}, it is common that iron will precipitate as iron sludge. Consequently, the recyclability of Fe^{3+}/ Fe^{2+} becomes a challenge issue as it is common in iron based Fenton reaction [92]. The sludge starts to form at a pH value of 4.

Table 2.2 includes different metal peroxides with the corresponding active oxygen content generated in aqueous media.

Table 2.2. Comparison of active oxygen content and purity of different oxidants

Oxidant	Molecular formula	Purity (wt%)	Active oxygen content wt %	References
Magnesium peroxide	MgO_2	94.26	26.93	[93]
Calcium peroxide	CaO_2	70	15.6	[94]

Zinc Peroxide	ZnO_2	73-80	12-13	[95]
Barium peroxide	BaO_2	95	9	[96]
Hydrogen peroxide	H_2O_2	30	14.1	[97]

Herein, a heterojunction of magnesium peroxide with CuAl-LDH was produced. It was synthesized through *in-situ* growth of magnesium peroxide nanoparticles on the surface of CuAl LDH using a reference as reported by Seftel *et al.*[14]. It works by taking the synergistic benefit of the LDH and metal peroxides. Initially the LDH adsorbs pollutants through electrostatic attraction followed by an ion exchanging capability. Then, magnesium peroxide generates hydrogen peroxide and then adsorbed pollutants are degraded through Fenton reaction mechanism.

3. MATERIALS AND METHODS

3.1. Chemicals and Reagents

All materials and reagents were used without further purifications. $Cu(NO_3)_2.3H_2O$, $Al(NO_3)_3.9H_2O$, NaOH, Na_2CO_3 (99%), 99.5% of isopropanol ($CH_3CHOHCH_3$), ammonium hydroxide (NH_4OH), $MgCl_2.6H_2O$, H_2SO_4, H_2O_2 (30%),10ppm of MO stock solution, 99.5% purity of ethylene diamine tetraacetic acid disodium salt or Na_2EDTA ($C_{10}H_{14}N_2Na_2O_8 \cdot 2H_2O$), and ethanol ($C_2H_5OH$, 99.9%) were used in this experimental work.

3.2. Apparatus and Instruments

Shimadzu XRD -7000 x - ray diffractometer determined with Cu Kα (λ=1.54056 Å) at a scanning rate of 4^0/min over 2θ of 10^0 to 80^0, magnetic stirrer, centrifuge, ultrasonicator, Fourier transform infrared spectroscopy with model of FTIR-6600 type A, scanning electron microscope (SEM, COXIEM-30), UV-Vis spectrometer of type UV-3600Plus Series. Silica glass beaker, test tube, pipettes, glove, pH meter, and volumetric flask were also used in this experimental work.

3.3. Synthesis of CuAl-LDH Catalysts

CuAl LDHs was synthesized through the co-precipitation method [98]. Typically, 15 mmol of Cu $(NO_3)_2.3H_2O$ and 7.5 mmol of Al $(NO_3)_2.3H_2O$ were dissolved in 100 mL distilled water. It was stirred for 2h with a molar ratio Cu to Al of 2:1. Under stirring, an aqueous solution of 1.2M Na_2CO_3 and 0.6M NaOH were dropped to the salt solution until pH becomes 9. Keeping the pH value 9, it was stirred at room temperature for another 10 h. Finally, precipitate was separated through filtration and washed with distilled water and ethanol. At the end, the as synthesized precipitate was dried at 70 ^{0}C for 20 h and CuAl-LDH powder was obtained.

3.4. Synthesis of MgO_2

Using *in-situ* growth method as reported on the literatures [99, 100], 10 mL of H_2O_2 was added to 2g $MgCl_2.6H_2O$ solution of 20 mL distilled water and stirred for 2h at room temperature. Then, 2M of NaOH was dropped until white foam formed and further stirred for 3h until the foam broken down. The milky white colored precipitate was aged for 18 h. Before it was dried at

100^0C with in 2h, the precipitate was washed with distilled water, ethanol, and finally with ammonia solution until pH reaches neutral.

3.4. Synthesis of CuAl-LDH/MgO_2 Composites

In a particular method, 0.35 g CuAl-LDH, 0.5 g CuAl-LDH and 0.65 g CuAl-LDH were added on different beakers containing 50mL distilled water. The measured amounts were dispersed at room temperature for 30 min to produce homogeneous suspension of (7, 10 and 13 $mgmL^{-1}$), respectively. Then, 2.36 g, 1.81g and 1.26 of $MgCl_2.6H_2O$ were added into the above suspension, respectively. The suspensions were further stirred for 1 h at room temperature. pH was adjusted to 12 using 25 mL of 2M NaOH for each suspensions. Keeping pH constant, 10 mL of H_2O_2 was dropped to each beaker and further stirred for another 4 h. The resulted mixtures were aged at room temperature for 16 h for better crystallinity. The obtained precipitates were washed with water and ethanol. At the end it was dried at 100 ^{0}C for 2h. Based on the mass concentration of CuAl-LDH (7, 10 and 13 $mgmL^{-1}$), the composite was labeled as CuAl-LDH/MgO_2-7, CuAl-LDH/MgO_2-10 and CuAl-LDH/MgO_2-13, respectively.

3.5. Characterization of the Catalyst

X-ray diffraction analysis was done using Shimadzu XRD -7000 diffractometer. Diffraction patterns was determined with Cu Kα (λ=1.54056 Å) at a scanning rate of 4^0/min over 2θ of 10^0 to 80^0. The measurement condition also runs with a voltage of 40kv, and 30mA. Scanning electron microscopy (SEM), COXIEM-30, was used to observe the surface structure of catalysts with the corresponding energy-dispersive X-ray spectroscopy (EDX) measurement for elemental analysis. XRD-7000, SEM, and UV-3600 Plus machines were South Korean made. Fourier transform infrared (FTIR-6600type A) analysis was conducted on different samples to investigate the composition and bonding status of functional groups. It was on the range of 399.19 to 4000 wavenumber (cm^{-1}) with a scanning speed of 2mm/sec.

3.6. Catalytic Degradation

The degradation of MO was determined by using Shimadzu–3600 Plus UV–Vis spectrophotometer in wavelength range of 200–800 nm. First 10ppm of 1000mL methyl orange stock solution was prepared. Then, 50 mL of 10ppm methyl orange (MO) solution was placed in a beaker. Subsequently, 20 mg of as-synthesized catalysts were added under neutral condition at room temperature. Under stirring, 5mL of the reaction solution was taken by plastic syringe at every 20min interval for measurement of residual concentration of MO. The concentration of MO was determined using UV-vis spectrometer.

4. RESULTS AND DISCUSSIONS

4.1. XRD Result Analysis

Figure 4.1, shows the XRD pattern of as-synthesized CuAl- LDH, MgO_2 and CuAl-LDH/MgO_2 composites. In detail, Figure 4.1a-e shows the pattern of MgO_2, CuAl- LDH, CuAl-LDH/MgO_2-7, CuAl-LDH/MgO_2-10 and CuAl-LDH/MgO_2-13 respectively. As evidenced by peaks on the XRD result, the amorphous nature of MgO_2 leads that MgO_2 rarely lay out on the diffraction peaks of CuAl-LDH/MgO_2 composite in a similar manner to article pointed out recently [57]. Consequently, the diffraction patterns of CuAl-LDH/MgO_2 resemble that of the CuAl-LDH patterns. The diffraction peaks of CuAl-LDH/MgO_2-7 gets minimum which is due to the lower content of LDH and the dominant phases of MgO_2 presented in that particular catalyst. The decrease in crystallinity is also an indicator of the non-regular arrangement of magnesium peroxide on the LDH. The typical diffraction peaks at 2θ value of 11.73^0, 23.59^0, 32.74^0, 35.47^0, 40.22^0, 47.97^0, and 60.3^0 corresponds to (300), (006), (009), (012), (015), (018), and (110) planes of hydrotalcite-like materials, respectively, (JCPDS card 37-630) [101]. The presence of several planes is a straightforward verification of higher crystallinity. It is a good justification of the inherited periodic interlayer of LDHs. The XRD patterns show the formation of the layered double hydroxide which is shortened as $Cu_6Al_2(OH)_{16}CO_3.4H_2O$. Moreover, the peaks at 11.73^0 is corresponds to carbonate (CO_3^{2-}) intercalated in the LDH. It is resulted from Na_2CO_3 as a precipitant in addition to CO_2 intercalation from the atmosphere. In Figure 4e, three broad peaks were also obtained at 37.2^0, 53.4^0 and 63.4^0 corresponding to (200), (220) and (311) planes of MgO_2, respectively, (JCPDS No.76-1363) [91]. The as-synthesized MgO_2 was pure at which there is no extra peaks corresponding to MgO and $Mg(OH)_2$ similar to a recent report [93]. The thickness of each peak is broader and shows smaller crystalline size. The crystalline size of the MgO_2 was calculated to 2.9nm, using Scherrer equation [14]. The lower crystalline size of magnesium peroxide leads to better dispersion upon forming a composite with the layered double hydroxide.

$$D = \frac{K\lambda}{\beta cos\theta} \quad \text{..... (1)}$$

Where, D is crystalline size, k is shape factor, λ is x-ray wavelength,

β is broadening at half maxima intensity (FWHM) and θ is Bragg's angle.

In general, the result reveals that LDHs allow other particles to grow with better dispersion. LDHs provide a site to grow magnesium peroxide along with inhibiting the irregular growth of MgO_2.

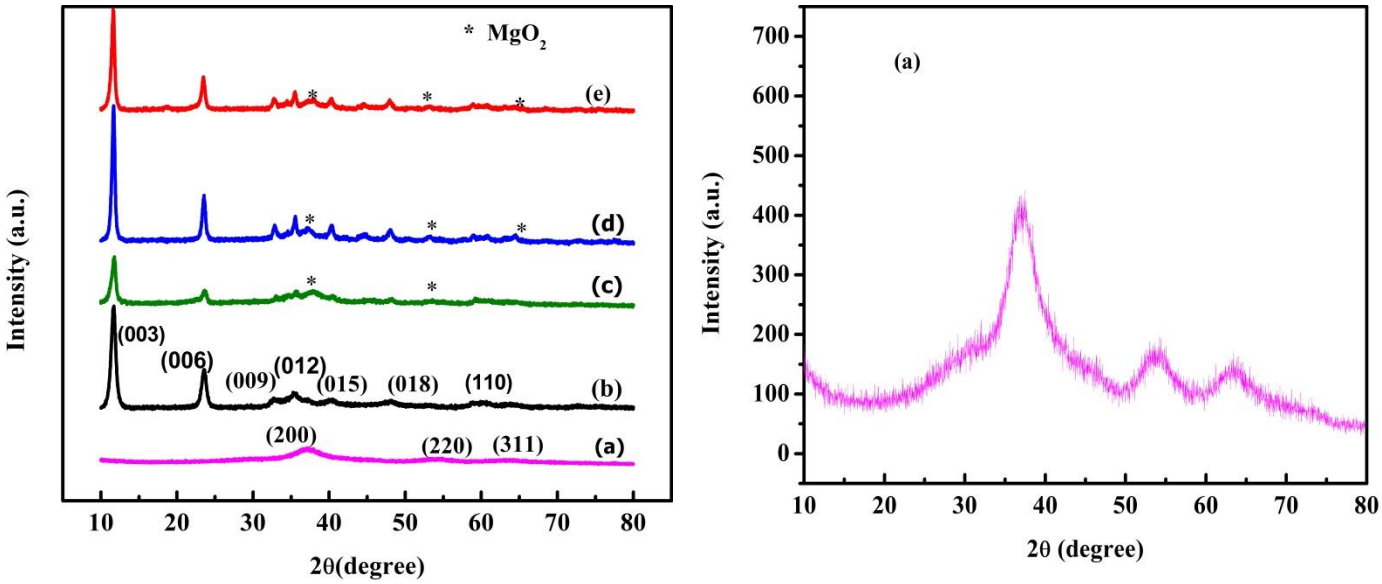

Figure 4.1. XRD patterns of (a) MgO_2; (b) CuAl-LDH; (c) CuAl-LDH/MgO_2-7; (d) CuAl-LDH/MgO_2-10 and (e) CuAl-LDH/MgO_2-13

4.2. SEM Analysis

Figure 4.2a–d also shows the scanning electron microscope (SEM) images of CuAl-LDH, MgO_2 and LDH/MgO_2-10 respectively and the corresponding SEM-energy-dispersive X-ray spectroscopy (SEM-EDX) of LDH/MgO_2-10 is also included. As shown in Figure 4.2a, flake like morphology was found for CuAl-LDH catalyst. While MgO_2 nanoparticles exhibit a cluster of particles as shown in Figure 4.2b. The presence of clustered particles is because of irregular growth implies that the as-synthesized MgO_2 nanoparticles have a large surface energy as common in small size nanoparticles. In response to its smaller crystalline size, pristine MgO_2 cannot bring well dispersion. However, based on Figure 4.2c, hardly detected any clustered particles when magnesium peroxide grows on the LDH. This could be due to magnesium peroxide particles are immobilized by the presence of LDH support. Hence, consistency of platelets in both CuAl-LDH and CuAl-LDH/MgO_2 is shown on the SEM micrographs. The very small crystalline size of MgO_2 particles may lead it to hardly saw on the SEM display unless backscattered SEM used. This is an indicator for the better correlation in between SEM analysis

and XRD justifications. SEM-EDX was used to evidence the presence of elements like Cu, Al, O, Mg, and C in CuAl-LDH/MgO_2 -10 as shown in Figure 4.2d. This study is well matched to other LDH based works [102]. Overall, SEM analysis has been well matched with the XRD conclusions saying that MgO_2 nanoparticles seldom displayed on the LDH sheet as well imposing negligible alteration on the LDH morphology despite non-precise structural analysis.

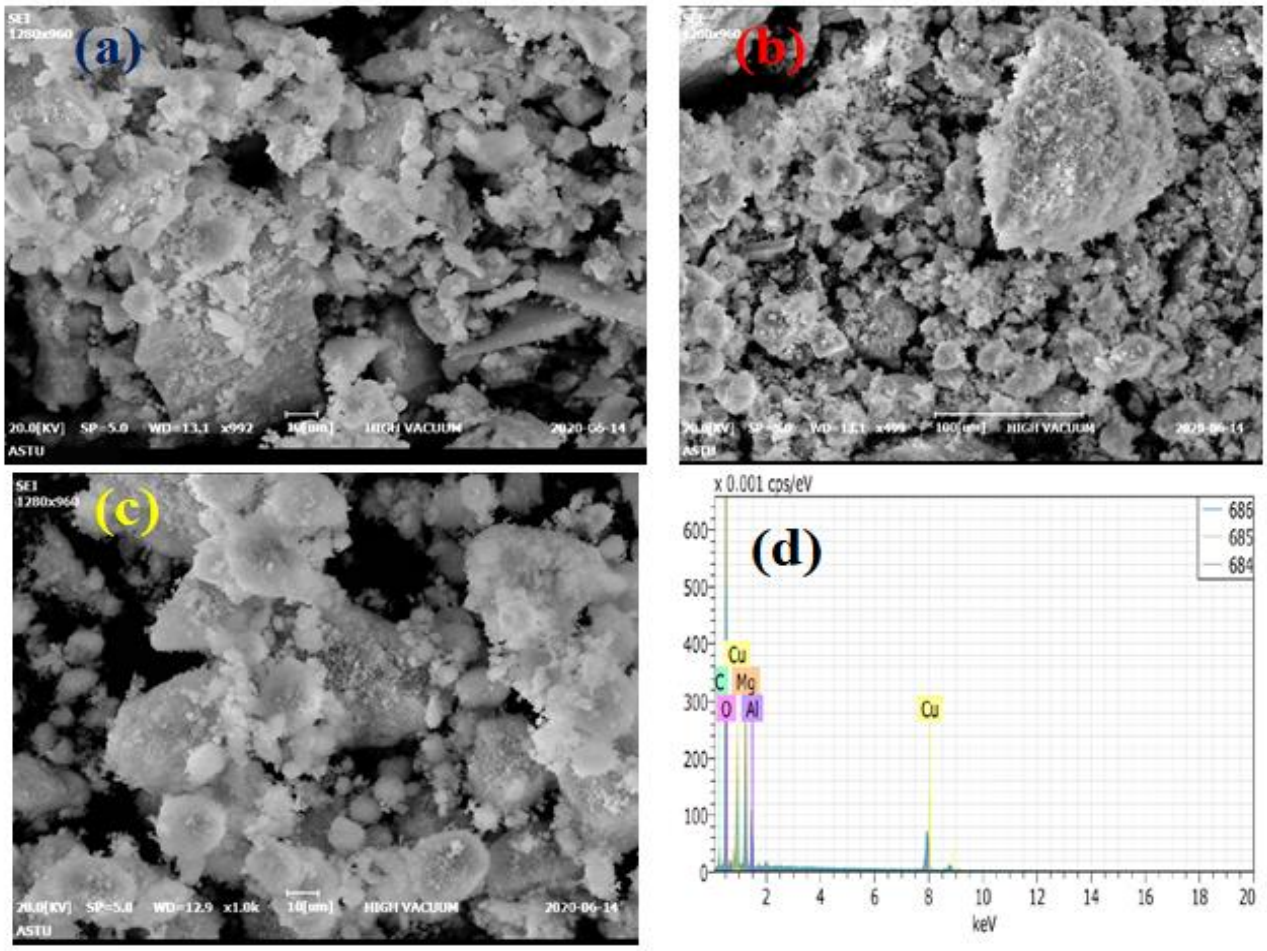

Figure 4.2. SEM images of (a) CuAl-LDH; (b) MgO_2; (c) CuAl-LDH/MgO_2-10; (d) EDX measurement of CuAl-LDH/MgO_2-10

4.3. FTIR Analysis

The composition and bonding status of functional groups are also examined by Fourier transform infrared spectroscopy (FTIR) analysis as shown below.

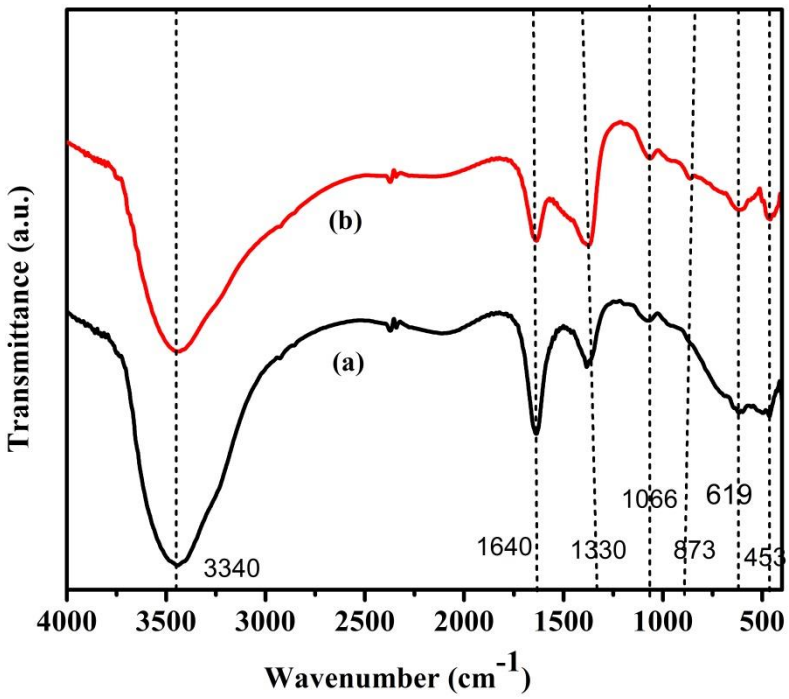

Figure 4.3. FTIR spectra of (a) CuAl-LDH; (b) CuAl-LDH/MgO_2-10

Figure 4.3 indicates the FTIR spectrum of CuAl- LDH and CuAl-LDH/MgO_2-10. The broad adsorption peak at 3340cm^{-1} attributed to the OH-stretching modes of interlayer water and hydroxyls together with bending modes at 1640cm^{-1}. The absorption peak at 1330cm^{-1} was associated to the v_3 vibration mode of CO_3^{2-}. The two weak absorbance bands at 1066 and 873 cm^{-1} indicate v_1 and v_2 modes of carbonate anions [51]. The weak absorption band at 619 and 453 wavenumbers were appeared due to the lattice vibration of metal oxygen (M–O, M–O–M and O–M–O groups). In the composite (curve b) OH stretching is relatively week while CO_3^{2-} vibrations are stronger than its vibration in the LDH. Generally, the presences of such vibrations demonstrate the intercalation of water molecules and carbonate ions into the interlayer spaces of CuAl–LDH.

4.4. Catalytic Activity

All the experiments were run at room temperature under dark condition. The catalytic performance of CuAl-LDH, MgO_2 and CuAl- LDH/MgO_2 composites were measured using UV-visible spectroscopy at a range of 200-800 nm wavelengths. Besides adsorption, there is no degradation shown by CuAl-LDH as shown in Figure 4.4b. In other word, once it reaches its maximum adsorption capacity for the incoming MO pollutant, it doesn't show any degradation [103]. Although the time has been prolonged to100min, no more difference on activity after 20min. Based on Figure 4.4a, MgO_2 by itself cannot perform well in the degradation of MO. Because without other reagents, peroxides hardly give rise to the formation of active species [100]. Rather it converts into harmless products like water. On the other hand, the composite form of MgO_2 and CuAl-LDH lead to both adsorption and degradation outcome as shown in Figure 4.4c-e. Among the composites, CuAl-LDH/MgO_2-7 shows minimum performance as shown in Figure 4.4c. It is because of poor dispersion of magnesium peroxide in addition to the minimum available copper to produce hydroxyl radicals. This can also be further confirmed by looking up the lower crystallinity of the LDH presented in that particular composition. The effect of different dosage of CuAl-LDH and MgO_2 on the composite was investigated upon decomposing methyl orange. Among the composites, maximum activity was obtained by CuAl-LDH/MgO_2-10 as shown in Figure 4.4d. This composition is attributed to the existence of both optimal copper and oxidant with a consequence of best catalytic activity.

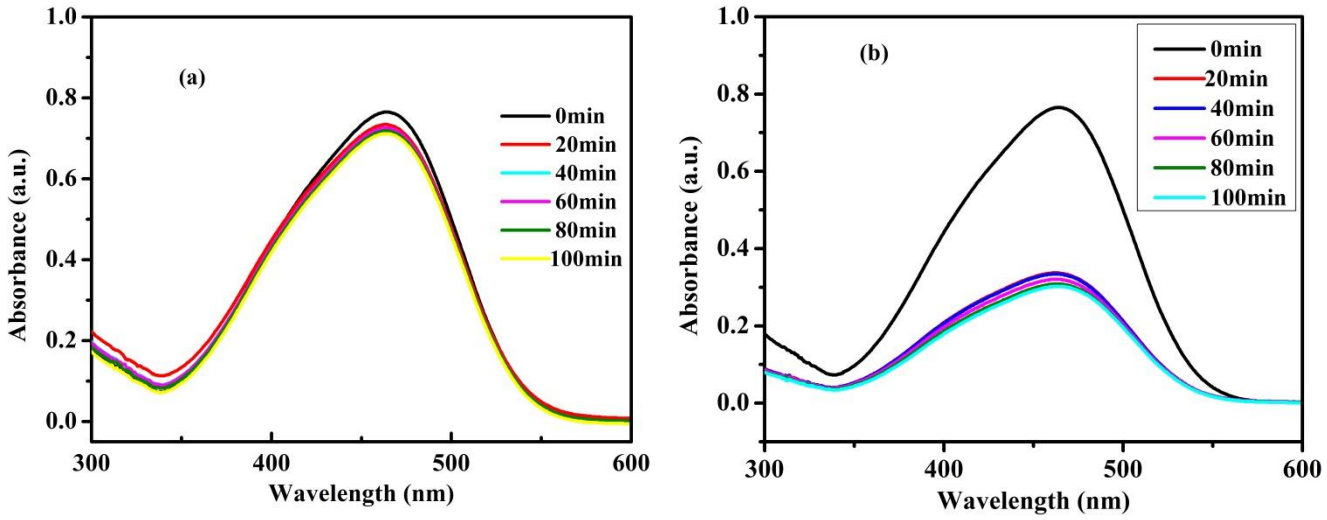

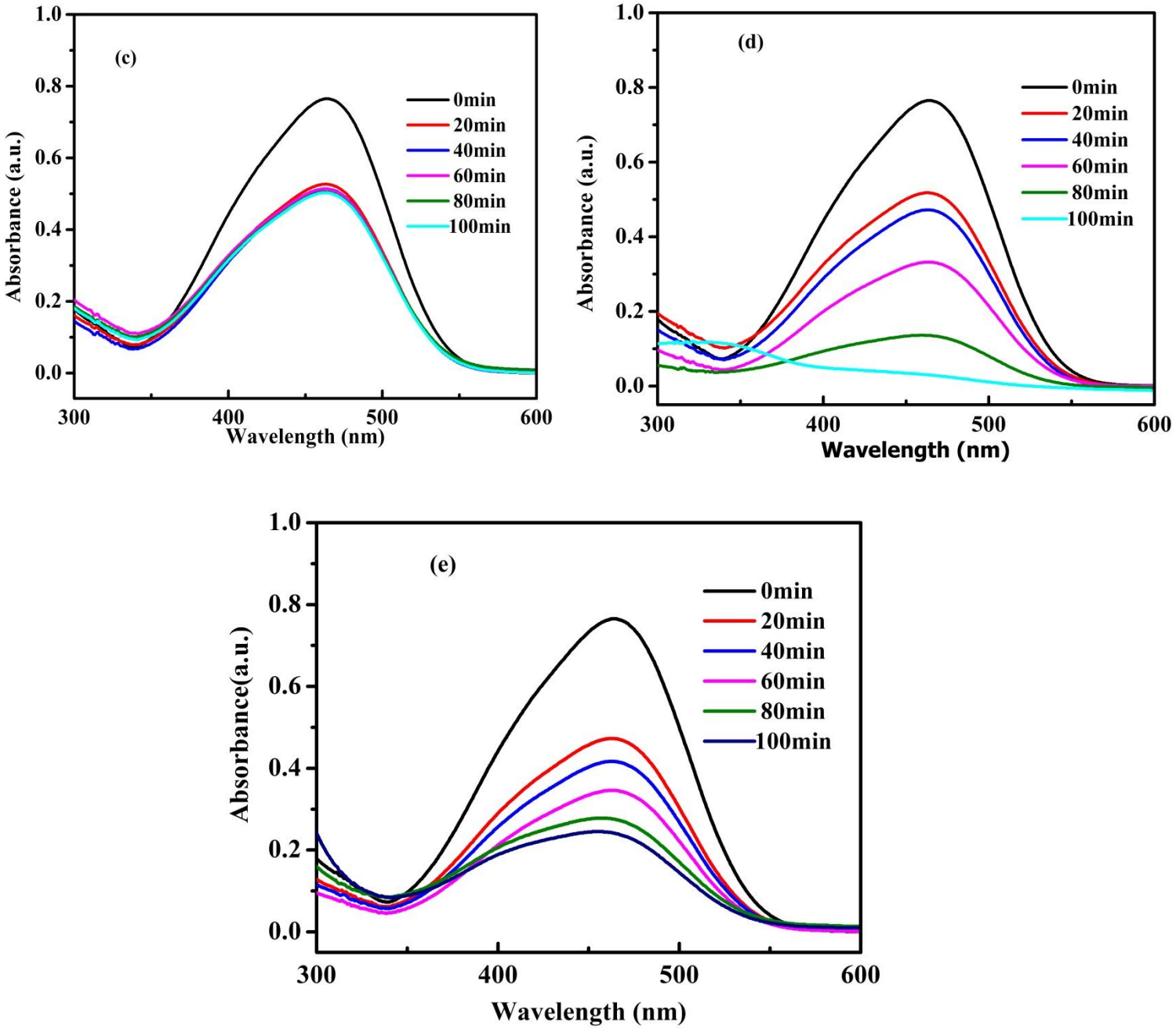

Figure 4.4. Absorbance versus wavelength patterns of (a) MgO_2; (b) CuAl-LDH; (C) CuAl-LDH/MgO_2-7; (d) CuAl-LDH/MgO_2-10 and (e) CuAl-LDH/MgO_2-13

The degradation efficiency of MO by CuAl-LDH/MgO_2-10 composite is highest after 100 min. This particular composition suggests that both copper and H_2O_2 are main components for the generation of optimal active oxygen species. On the other hand, CuAl-LDH/MgO_2-13 composite shows good performance next to CuAl- LDH/MgO_2-10 composite. It can be due to the higher copper content. Initially CuAl-LDH/MgO_2-13 performs well, but as time goes on it

doesn't work as CuAl- LDH/MgO_2-10. One reason may be the lowest peroxide generation due to the lower amount of MgO_2 in the LDH/MgO_2-13 composition. The degradation efficiency of MO is calculated by applying equation (2). As a result, 97% of MO initial concentration was degraded.

$$\% \text{ degradation} = (1-C_t/C_o) \times 100 \quad \ldots\ldots (2)$$

Where C_o is initial pollutant concentration & C_t is the concentration of pollutant at some time't'

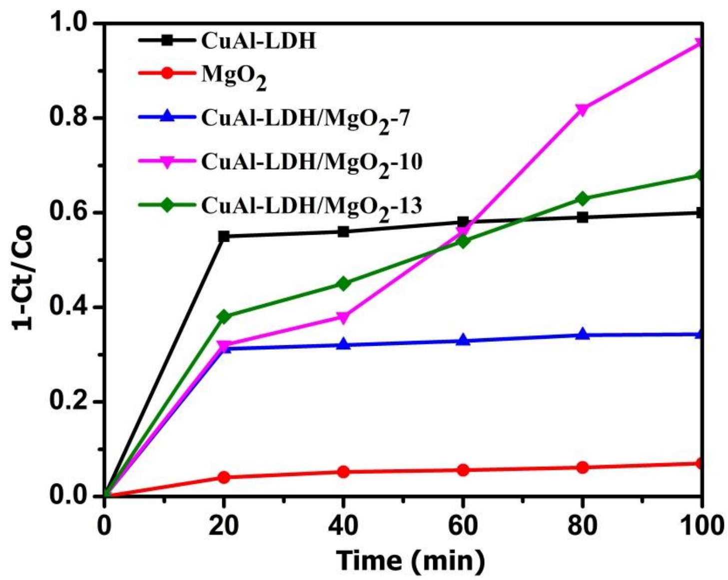

Figure 4.5. Percentage removal versus time graph.

Generally, by realizing the composition of synthesized samples and the above performance graphs, it is possible to deduce as follow. In addition to obtaining enough H_2O_2 from MgO_2 in aqueous media, it is the higher content of copper that can able to generate more ROS thereby degrading peroxides.

4.5. Effect of pH

pH effect is an essential parameter for the oxidation potential of •OH radicals [104]. Experiments were done for acid and neutral condition to realize initial pH effect. The pH was adjusted by using 0.01 M of H_2SO_4 and 0.01M NaOH. As shown in Figure 4.6, the degradation of MO was higher at pH value of 3.6 than in neutral state. At lower pH, adsorption of negatively charged MO gets intensified due to positively charged catalyst surface of the LDH. Besides that, it is because of hydroxide radicals which have higher power to oxidize pollutants in acidic media.

Thus, more hydroxyl radicals form at low pH along with enhancing degradation efficiency [105]. While at higher pH, there is a competition between OH ion and methyl orange for the same site of positively charged LDH layer. As a result, performance gets lower and lower relative to the acidic media as there will be less adsorbed MO to be degraded by radicals.

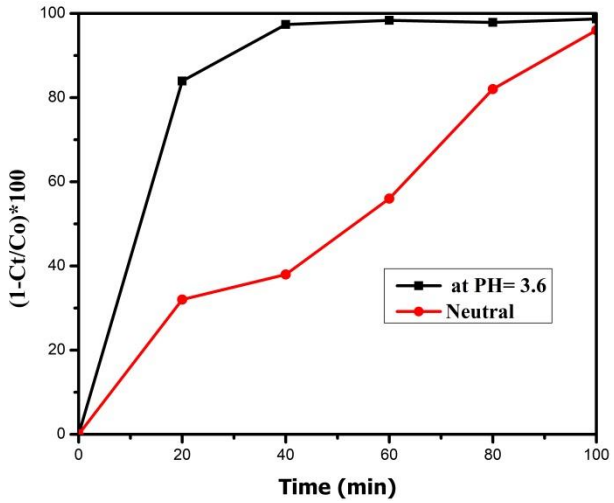

Figure 4.6. Effect of initial pH on MO degradation using CuAl-LDH/MgO_2-10

4.6. Trapping Experiments

To investigate the need of active oxygen species, Na_2EDTA was used as transition metal chelator , and isopropanol as hydroxyl radical quencher [106]. Typically, 10mM Na_2EDTA and 0.2 mL of isopropanol (10mM) were separately added to 200 mL of 10 ppm of MO solution followed by adding 0.0895g of LDH/MgO_2 -10 catalyst. As depicted in Figure 4.7, the presence of Na_2EDTA grabs or chelates copper so that adsorption gets minimized. In turn, it has antioxidant property and free radical quenching activity. Besides grabbing copper, Na_2EDTA can also indirectly act as scavenger of ROS thereby reducing the available copper and decreasing the formation of •OH obtained by Fenton reaction system [107]. The residual concentration of MO is close to zero without scavengers within 100min. When scavengers exist, concentration versus time values exhibit a little change. This result suggests that both copper and •OH play basic role for the degradation of methyl orange.

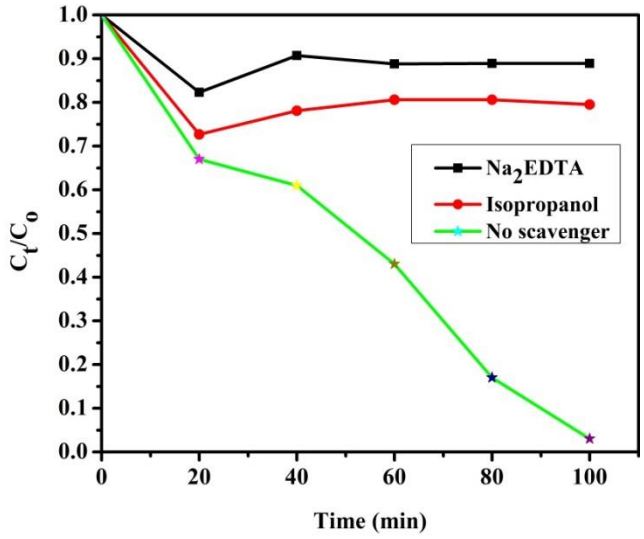

Figure 4.7. Radical quenching effect on MO degradation using CuAl-LDH/MgO_2-10

4.7. Kinetics of MO dye degradation

Figure 4.8 a shows the degradation kinetics of MO by different catalysts with time. The first order rate constant for an optimal MO degradation is 3.14×10^{-2} min^{-1} (Table 4.1). The rate constant of CuAl-LDH/MgO_2-10 is 4.4 and 44.8 times larger than CuAl-LDH and MgO_2 respectively. The regression coefficient values corresponding to each catalyst is also listed in Table 4.1. It tells how good each data's correlate one another. First order reaction is conveyed by equation (3) and the resulting values are tabulated as listed in Table 4.1.

$$\ln(C_t/C_o) = -K_1 t \quad \ldots\ldots (3)$$

Where, C_o is initial concentration and C_t concentration of MO at a reaction time t

K_1 is Pseudo-first kinetics rate constant

Table 4.1. First order rate constant for MO

Composition	$K_1(min^{-1})x1o^{-2}$	R^2, for first order	R^2, for second order
CuAl-LDH	0.72	0.98	0.99
MgO_2	0.07	0.83	0.83
LDH/MgO_2-7	0.32	0.92	0.92
LDH/MgO_2-10	3.14	0.84	0.78
LDH/MgO_2-13	1.08	0.99	0.97

Other authors also reported that the degradation of dyes under Fenton reaction follows pseudo-first-order [104, 108].

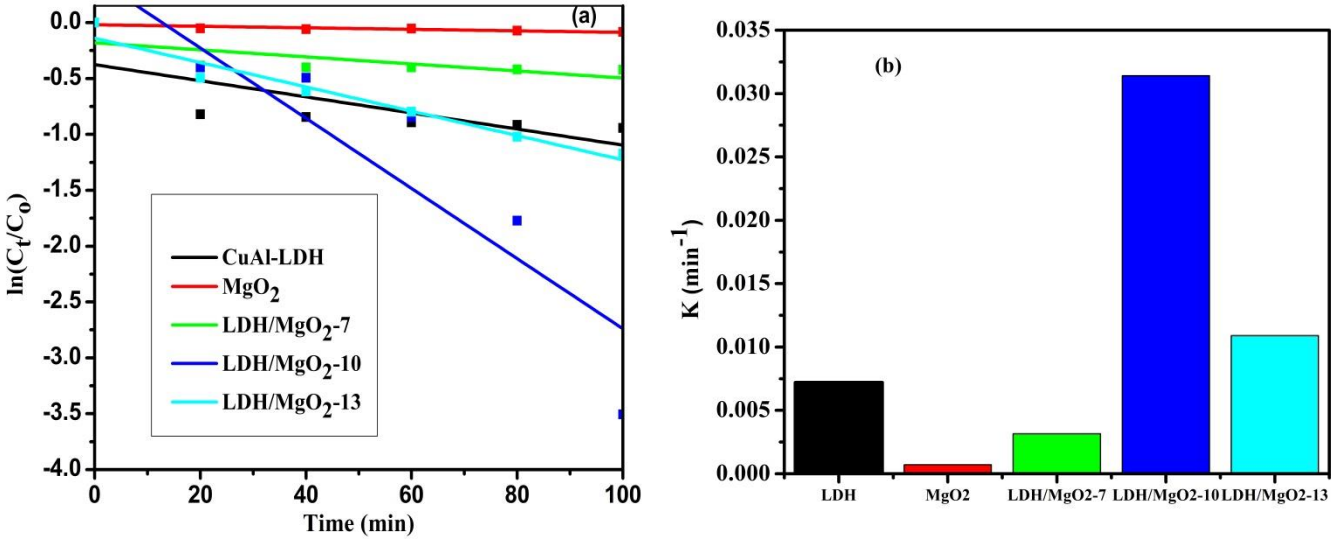

Figure 4.8. (a) degradation kinetics of MO by different catalysts and (b) bar diagram plot of rate constant values for different catalysts

4.8. Re-usability Test

The stability of the catalyst is an important factor for practical usage. In this work, the stability was evaluated by running four cycles. Typically 200 mg of CuAl-LDH/MgO_2-10 catalyst was added into 500 mL of 10 ppm methyl orange solution. After 100 min, the first run was ended up and followed by allowing catalyst to settle for 2h. Then, the catalyst was filtered

and re-used for the next remain runs. The difficulty in transporting hydrogen peroxide upon conducting Fenton reaction has been remained as a common challenge. In earlier work, Li *et al.* stated that CuAl-LDH for MO degradation doesn't show persistent activity for multiple run [51]. In this work, the recyclability of as synthesized catalyst is very high relative to earlier studies on degradation of MO by LDH despite consuming time. As H_2O_2 generated in-situ way, it shows consistent activity for multiple runs. Furthermore, the XRD diffiracton patterns after proceeding cylic runs resembles the pattern of the composite before a reaction. This further pinpoints the better stability owned by the as-synthesised composite.

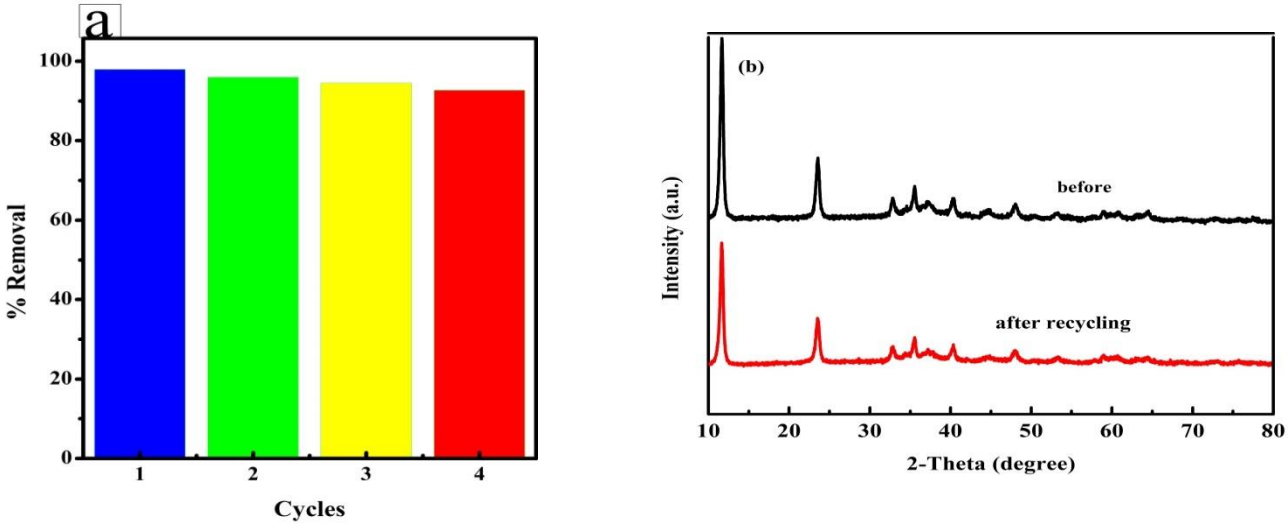

Figure 4.9. (a) Re-usability and (b) XRD of CuAl-LDH/MgO_2 -10 before and after cyclic test.

4.9. Degradation Mechanism

Initially MO pollutants adsorbed by the catalyst through electrostatic attraction. Under aqueous media magnesium peroxide starts to generate hydrogen peroxide while copper from the hydrotalcite layer converts the generated peroxide into active oxygen species. Once those active species formed, MO starts to decompose into non-toxic products like CO_2, and H_2O. The generation of •OH through Fenton reaction is dependent on the content of available reagent and peroxide.

Hydrogen peroxide generation mechanism and degradation process can be described by the following equations.

$$MgO_2 + H_2O \rightleftharpoons MgO + H_2O_2 \quad (4.4)$$

$$H_2O_2 + Cu^{1+} \longrightarrow \bullet OH + OH^- + Cu^{2+} \quad (4.5)$$

$$Cu^{2+} + H_2O_2 \longrightarrow Cu^{1+} + \bullet HO_2 + H^+ \quad (4.6)$$

$$\bullet OH + H_2O_2 \longrightarrow \bullet HO_2 + H_2O \quad (4.7)$$

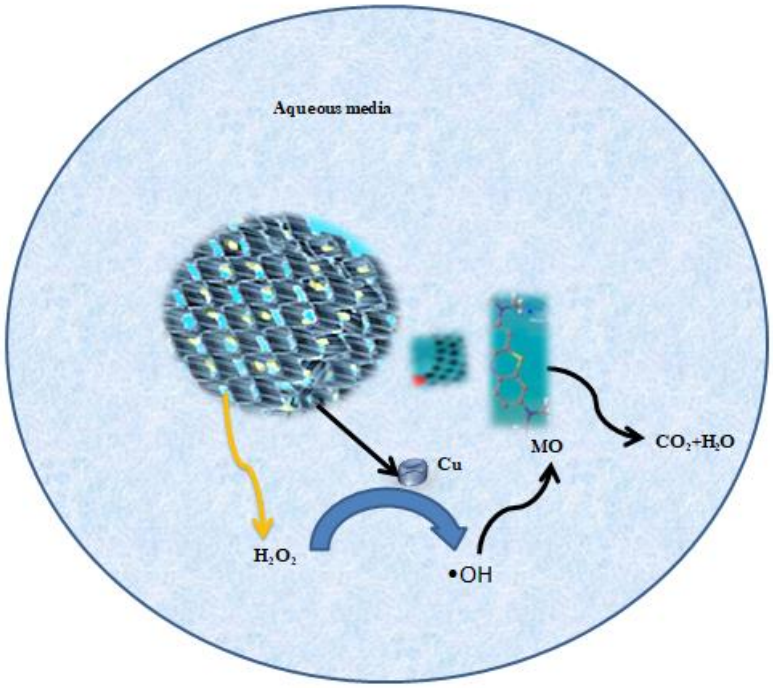

Figure 4.10. Schematic diagram of catalysis to degrade MO

5. CONCLUSION

In summary, a new catalyst is fabricated through in-situ growth of magnesium peroxide on the LDH sheet. Basically, a modified pathway of the conventional Fenton reaction process is used. Under aqueous media and dark environment, the as synthesized catalyst itself able to produce an oxidant. Consequently, it is less economical in comparison to photo Fenton process which always needs a light irradiation. The as-synthesized catalyst was analyzed with different characterization tools with a result of good correlation. For instance the amorphous nature of magnesium peroxide shows poor crystallinity as depicted in the XRD graphs. Likewise, owing to the smaller size of magnesium peroxide, it barely alters XRD peaks and the morphology of the composite isn't precisely determined using SEM. Furthermore, FTIR confirms the formation of hydrotalcite. Hence the presence of CO_3^{2-}, and ^{-}OH indicates the intercalation of water molecules and carbonate ions into the interlayer spaces of LDH. Besides that, as cross checked by EDX analysis of LDH/MgO_2-10 catalyst and trapping experiments, it is the higher content of copper that plays the major role for the degradation of MO. The essentiality of both copper and hydroxyl radical are just well confirmed by running trapping experiments. In doing so activity is suppressed in response to the existence of both scavengers. Both LDH and MgO_2 catalysts alone don't show continuous improvement even though reaction time increases as seen in concentration versus time plot. While their composite forms leads enhanced activity which is a good implication to the synergistic outcome from each individual. The composite catalysts bring persistent improvement thereby adsorbing and also through degradation in response to the generated hydroxyl radical. On the other hand when pH decreased to acidic range (3.6), the removal efficiency of MO is increased from 32% to 83% within 20min. This is attributed to an optimum adsorption of negatively charged MO by LDHs when reaction proceeds at acidic range. But, acidic media leads to secondary disposal treatment and leaching of catalyst parts as a result reusability will become difficult. Generally, a new insight for overcoming external chemical supply together with eliminating the requirement of a short pH range was obtained.

6. RECOMMENDATIONS

Realizing the unique properties of LDHs, it is better to further work on dealing with synthesizing LDH based composites.

- Rather than magnesium peroxide, it is better to find out other metal peroxides which can able to worth a dual function, meaning generating peroxide as well producing hydroxyl radicals.
- For optimal performance, not only peroxides but also enough content of a reagent that converts peroxide into hydroxyl radical is required.

7. REFERENCES

[1] E. Dvininov, M. Ignat, P. Barvinschi, M. Smithers, E. Popovici, New SnO_2/MgAl-layered double hydroxide composites as photocatalysts for cationic dyes bleaching, Journal of hazardous materials, 177 (2010) 150-158.

[2] K.H. O, E.J. Rupa, G. Anandapadmanaban, M. Chokkalingam, J.F. Li, J. Markus, V. Soshnikova, Z.E.J. Perez, D.-C. Yang, Cationic and anionic dye degradation activity of Zinc oxide nanoparticles from Hippophae rhamnoides leaves as potential water treatment resource, Optik, 181 (2019) 1091-1098.

[3] M.A.R. Cardenas, I. Ali, F.Y. Lai, L. Dawes, R. Thier, J. Rajapakse, Removal of micropollutants through a biological wastewater treatment plant in a subtropical climate, Queensland-Australia, Journal of Environmental Health Science and Engineering, 14 (2016) 14.

[4] R.D.C. Soltani, S. Jorfi, H. Ramezani, S. Purfadakari, Ultrasonically induced ZnO–biosilica nanocomposite for degradation of a textile dye in aqueous phase, Ultrasonics sonochemistry, 28 (2016) 69-78.

[5] S. Mustapha, M. Ndamitso, A. Abdulkareem, J. Tijani, D. Shuaib, A. Ajala, A. Mohammed, Application of TiO_2 and ZnO nanoparticles immobilized on clay in wastewater treatment: a review, Applied Water Science, 10 (2020) 1-36.

[6] P. Garcia-Muñoz, F. Fresno, C. Lefevre, D. Robert, N. Keller, Synergy effect between photocatalysis and heterogeneous photo-Fenton catalysis on Ti-doped $LaFeO_3$ perovskite for high efficiency light-assisted water treatment, Catalysis Science & Technology, 10 (2020) 1299-1310.

[7] Y. Wan, J. Wang, F. Huang, Y. Xue, N. Cai, J. Liu, W. Chen, F. Yu, Synergistic effect of adsorption coupled with catalysis based on graphene-supported MOF hybrid aerogel for promoted removal of dyes, RSC advances, 8 (2018) 34552-34559.

[8] F. Opoku, E.M. Kiarii, P.P. Govender, M.A. Mamo, Metal Oxide Polymer Nanocomposites in Water Treatments, Descriptive Inorganic Chemistry Researches of Metal Compounds, Intech Open 2017.

[9] H. Zhang, G. Li, L. Deng, H. Zeng, Z. Shi, Heterogeneous activation of hydrogen peroxide by cysteine intercalated layered double hydroxide for degradation of organic pollutants: Performance and mechanism, Journal of colloid and interface science, 543 (2019) 183-191.

[10] G.K. Cheruiyot, W.C. Wanyonyi, J.J. Kiplimo, E.N. Maina, Adsorption of toxic crystal violet dye using coffee husks: Equilibrium, kinetics and thermodynamics study, Scientific African, 5 (2019) e00116.
[11] A.M. Golsheikh, K.Z. Kamali, N.M. Huang, A.K. Zak, Effect of calcination temperature on performance of ZnO nanoparticles for dye-sensitized solar cells, Powder Technology, 329 (2018) 282-287.
[12] H. Lu, Z. Zhu, H. Zhang, J. Zhu, Y. Qiu, L. Zhu, S. Küppers, Fenton-like catalysis and oxidation/adsorption performances of acetaminophen and arsenic pollutants in water on a multimetal Cu–Zn–Fe-LDH, ACS applied materials & interfaces, 8 (2016) 25343-25352.
[13] B. Ali, B. Naceur, E. Abdelkader, E. Karima, B. Nourredine, Competitive adsorption of binary dye from aqueous solutions using calcined layered double hydroxides, International Journal of Environmental Analytical Chemistry, (2020) 1-20.
[14] E. Seftel, M. Puscasu, M. Mertens, P. Cool, G. Carja, Assemblies of nanoparticles of CeO_2–ZnTi-LDHs and their derived mixed oxides as novel photocatalytic systems for phenol degradation, Applied Catalysis B: Environmental, 150 (2014) 157-166.
[15] E. Brillas, S. Garcia-Segura, Benchmarking recent advances and innovative technology approaches of Fenton, photo-Fenton, electro-Fenton, and related processes: A review on the relevance of phenol as model molecule, Separation and Purification Technology, 237 (2020) 116337.
[16] A. Asghar, A.A.A. Raman, W.M.A.W. Daud, Advanced oxidation processes for in-situ production of hydrogen peroxide/hydroxyl radical for textile wastewater treatment: a review, Journal of cleaner production, 87 (2015) 826-838.
[17] A.D. Bokare, W. Choi, Review of iron-free Fenton-like systems for activating H_2O_2 in advanced oxidation processes, Journal of hazardous materials, 275 (2014) 121-135.
[18] J. Ma, N. Jia, C. Shen, W. Liu, Y. Wen, Stable cuprous active sites in Cu^+-graphitic carbon nitride: Structure analysis and performance in Fenton-like reactions, Journal of hazardous materials, 378 (2019) 120782.
[19] Y. Zhang, B. Wu, H. Xu, H. Liu, M. Wang, Y. He, B. Pan, Nanomaterials-enabled water and wastewater treatment, NanoImpact, 3 (2016) 22-39.
[20] A.M. Briggs, M.J. Cross, D.G. Hoy, L. Sanchez-Riera, F.M. Blyth, A.D. Woolf, L. March, Musculoskeletal health conditions represent a global threat to healthy aging: a report for the 2015

World Health Organization world report on ageing and health, The Gerontologist, 56 (2016) S243-S255.
[21] R. Kant, Textile dyeing industry an environmental hazard, (2011).
[22] K. Umar, M.N.M. Ibrahim, A. Ahmad, M. Rafatullah, Synthesis of Mn-doped TiO_2 by novel route and photocatalytic mineralization/intermediate studies of organic pollutants, Research on Chemical Intermediates, 45 (2019) 2927-2945.
[23] K. Konieczny, M. Bodzek, M. Rajca, A coagulation–MF system for water treatment using ceramic membranes, Desalination, 198 (2006) 92-101.
[24] W.-W. Tang, G.-M. Zeng, J.-L. Gong, J. Liang, P. Xu, C. Zhang, B.-B. Huang, Impact of humic/fulvic acid on the removal of heavy metals from aqueous solutions using nanomaterials: a review, Science of the total environment, 468 (2014) 1014-1027.
[25] X. Qu, J. Brame, Q. Li, P.J. Alvarez, Nanotechnology for a safe and sustainable water supply: enabling integrated water treatment and reuse, Accounts of chemical research, 46 (2013) 834-843.
[26] A.A. Yaqoob, T. Parveen, K. Umar, M.N. Mohamad Ibrahim, Role of nanomaterials in the treatment of wastewater: A review, Water, 12 (2020) 495.
[27] T. Mano, S. Nishimoto, Y. Kameshima, M. Miyake, Water treatment efficacy of various metal oxide semiconductors for photocatalytic ozonation under UV and visible light irradiation, Chemical Engineering Journal, 264 (2015) 221-229.
[28] D. Chen, Z. Wang, T. Ren, H. Ding, W. Yao, R. Zong, Y. Zhu, Influence of Defects on the Photocatalytic Activity of ZnO, The Journal of Physical Chemistry C, 118 (2014) 15300-15307.
[29] T.C. Madzokere, A. Karthigeyan, Heavy metal ion effluent discharge containment using magnesium oxide (MgO) Nanoparticles, Materials Today: Proceedings, 4 (2017) 9-18.
[30] C. Belver, C. Han, J. Rodriguez, D. Dionysiou, Innovative W-doped titanium dioxide anchored on clay for photocatalytic removal of atrazine, Catalysis Today, 280 (2017) 21-28.
[31] J. Kulkarni, R. Ravishankar, H. Nagabhushana, K. Ananthraju, R. Basavraj, L. Renuka, Green Synthesis of Ni-Doped Magnesium Oxide Nanoparticles and its Effect on Photo Catalysis, Indian Journal of Advances in Chemical Science S1, 64 (2016) 67.
[32] Y. Cai, D. Wu, X. Zhu, W. Wang, F. Tan, J. Chen, X. Qiao, X. Qiu, Sol-gel preparation of Ag-doped MgO nanoparticles with high efficiency for bacterial inactivation, Ceramics International, 43 (2017) 1066-1072.

[33] B. Shahmoradi, F. Farahani, S. Kohzadi, A. Maleki, M. Pordel, Y. Zandsalimi, Y. Gong, J. Yang, G. McKay, S.-M. Lee, Application of cadmium-doped ZnO for the solar photocatalytic degradation of phenol, Water Science and Technology, 79 (2019) 375-385.
[34] R. Kumar, S. Anandan, K. Hembram, T.N. Rao, Efficient ZnO-based visible-light-driven photocatalyst for antibacterial applications, ACS Appl Mater Interfaces, 6 (2014) 13138-13148.
[35] D. Lehr, M. Luka, M.R. Wagner, M. Bügler, A. Hoffmann, S. Polarz, Band-Gap Engineering of Zinc Oxide Colloids via Lattice Substitution with Sulfur Leading to Materials with Advanced Properties for Optical Applications Like Full Inorganic UV Protection, Chemistry of Materials, 24 (2012) 1771-1778.
[36] A. Torabi, V.N. Staroverov, Band Gap Reduction in ZnO and ZnS by Creating Layered ZnO/ZnS Heterostructures, J Phys Chem Lett, 6 (2015) 2075-2080.
[37] R.X. Chen, S.L. Zhu, J. Mao, Z.D. Cui, X.J. Yang, Y.Q. Liang, Z.Y. Li, Synthesis of CuO/Co_3O_4 Coaxial Heterostructures for Efficient and Recycling Photodegradation, International Journal of Photoenergy, 2015 (2015) 1-11.
[38] G. Mohamed Reda, H. Fan, H. Tian, Room-temperature solid state synthesis of Co_3O_4/ZnO p–n heterostructure and its photocatalytic activity, Advanced Powder Technology, 28 (2017) 953-963.
[39] S. Wu, X. Shen, G. Zhu, H. Zhou, Z. Ji, K. Chen, A. Yuan, Synthesis of ternary $Ag/ZnO/ZnFe_2O_4$ porous and hollow nanostructures with enhanced photocatalytic activity, Applied Catalysis B: Environmental, 184 (2016) 328-336.
[40] Z. Li, H. Chen, W. Liu, Full-Spectrum Photocatalytic Activity of $ZnO/CuO/ZnFe_2O_4$ Nanocomposite as a PhotoFenton-Like Catalyst, Catalysts, 8 (2018) 557.
[41] L. Zhang, Z. Xiong, G. Zhao, Chapter 13. Hierarchical Nanoheterostructures: Layered Double Hydroxide-based Photocatalysts, (2015) 309-338.
[42] J. Ma, P. Duan, D. Ren, W. Zhou, Effects of layered double hydroxides incorporation on carbonation resistance of cementitious materials, Journal of Materials Research and Technology, 8 (2019) 292-298.
[43] G. Fan, F. Li, D.G. Evans, X. Duan, Catalytic applications of layered double hydroxides: recent advances and perspectives, Chem Soc Rev, 43 (2014) 7040-7066.
[44] X. Bi, H. Zhang, L. Dou, Layered double hydroxide-based nanocarriers for drug delivery, Pharmaceutics, 6 (2014) 298-332.

[45] X. Peng, M. Wang, F. Hu, F. Qiu, T. Zhang, H. Dai, Z. Cao, Multipath fabrication of hierarchical CuAl layered double hydroxide/carbon fiber composites for the degradation of ammonia nitrogen, Journal of Environmental Management, 220 (2018) 173-182.
[46] F. Zhao, L. Fan, K. Xu, D. Hua, G. Zhan, S.-F. Zhou, Hierarchical sheet-like Cu/Zn/Al nanocatalysts derived from LDH/MOF composites for CO_2 hydrogenation to methanol, Journal of CO_2 Utilization, 33 (2019) 222-232.
[47] N.S. Ahmed, R. Menzel, Y. Wang, A. Garcia-Gallastegui, S.M. Bawaked, A.Y. Obaid, S.N. Basahel, M. Mokhtar, Graphene-oxide-supported CuAl and CoAl layered double hydroxides as enhanced catalysts for carbon-carbon coupling via Ullmann reaction, Journal of Solid State Chemistry, 246 (2017) 130-137.
[48] G. Fan, F. Li, D.G. Evans, X. Duan, Catalytic applications of layered double hydroxides: recent advances and perspectives, Chem. Soc. Rev., 43 (2014) 7040-7066.
[49] Y.-T. Hsu, J.C.S. Wu, V.-H. Nguyen, Mg_xAl-LDHs layered double hydroxides catalysts for boosting catalytic synthesis of biodiesel and conversion of by-product into valuable glycerol carbonate, Journal of the Taiwan Institute of Chemical Engineers, 104 (2019) 219-226.
[50] H. Jia, Y. Zhao, P. Niu, N. Lu, B. Fan, R. Li, Amine-functionalized MgAl LDH nanosheets as efficient solid base catalysts for Knoevenagel condensation, Molecular Catalysis, 449 (2018) 31-37.
[51] J. Li, S. Zhang, Y. Chen, T. Liu, C. Liu, X. Zhang, M. Yi, Z. Chu, X. Han, A novel three-dimensional hierarchical CuAl layered double hydroxide with excellent catalytic activity for degradation of methyl orange, RSC Advances, 7 (2017) 29051-29057.
[52] L. Cao, Y. Ma, A. Song, L. Bai, P. Zhang, X. Li, G. Shao, Stable composite of flower-like NiFe-layered double hydroxide nucleated on graphene oxide as an effective catalyst for oxygen reduction reaction, Int. J. Hydrogen Energy, 44 (2019) 5912-5920.
[53] S. Zhao, H. Zhu, Z. Wang, P. Song, M. Ban, X. Song, A loose hybrid nanofiltration membrane fabricated via chelating-assisted in-situ growth of Co/Ni LDHs for dye wastewater treatment, Chem. Eng. J., 353 (2018) 460-471.
[54] X. Tao, Y. Han, C. Sun, L. Huang, D. Xu, Plasma modification of NiAlCe–LDH as improved photocatalyst for organic dye wastewater degradation, Applied Clay Science, 172 (2019) 75-79.

[55] J. Wu, Y. Gong, Q. Fu, C. Pan, NiFe-LDH@ ZnO@ NF composite for photo-degradation of Rhodamine B dye, MRS Advances, 4 (2019) 1887-1893.
[56] E. Mustafa, A. Tahira, R.E. Adam, Z.H. Ibupoto, S. Elhag, M. Willander, O. Nur, Efficient Ni–Fe layered double hydroxides/ZnO nanostructures for photochemical water splitting, Journal of Solid State Chemistry, 273 (2019) 186-191.
[57] W. Zheng, S. Sun, Y. Xu, R. Yu, H. Li, Facile synthesis of NiAl-LDH/MnO_2 and NiFe-LDH/MnO_2 composites for high-performance asymmetric supercapacitors, Journal of Alloys and Compounds, 768 (2018) 240-248.
[58] S. Nayak, K. Parida, Nanostructured CeO_2/MgAl-LDH composite for visible light induced water reduction reaction, International Journal of Hydrogen Energy, 41 (2016) 21166-21180.
[59] R. Lu, X. Xu, J. Chang, Y. Zhu, S. Xu, F. Zhang, Improvement of photocatalytic activity of TiO_2 nanoparticles on selectively reconstructed layered double hydroxide, Applied Catalysis B: Environmental, 111 (2012) 389-396.
[60] Y. Zhi, Y. Li, Q. Zhang, H. Wang, ZnO nanoparticles immobilized on flaky layered double hydroxides as photocatalysts with enhanced adsorptivity for removal of acid red G, Langmuir, 26 (2010) 15546-15553.
[61] T. Kameda, T. Yoshioka, J. Cuppoletti, Hybrid inorganic/organic composites of layered double hydroxides intercalated with organic acid anions for the uptake of hazardous substances from aqueous solution, Metal, ceramic and polymeric composites for various uses, (2011) 123-148.
[62] J. Zhang, F. Zhang, L. Ren, D.G. Evans, X. Duan, Synthesis of layered double hydroxide anionic clays intercalated by carboxylate anions, Materials Chemistry and Physics, 85 (2004) 207-214.
[63] V. Prevot, Y. Tokudome, 3D hierarchical and porous layered double hydroxide structures: an overview of synthesis methods and applications, Journal of Materials Science, 52 (2017) 11229-11250.
[64] X. Wu, D. Zhang, F. Jiao, S. Wang, Visible-light-driven photodegradation of Methyl Orange using Cu_2O/ZnAl calcined layered double hydroxides as photocatalysts, Colloids and Surfaces A: Physicochemical and Engineering Aspects, 508 (2016) 110-116.

[65] J.S. Valente, F. Tzompantzi, J. Prince, Highly efficient photocatalytic elimination of phenol and chlorinated phenols by CeO_2/MgAl layered double hydroxides, Applied Catalysis B: Environmental, 102 (2011) 276-285.
[66] S. Bai, X. Yang, C. Liu, X. Xiang, R. Luo, J. He, A. Chen, An integrating photoanode of WO_3/Fe_2O_3 heterojunction decorated with NiFe-LDH to improve PEC water splitting efficiency, ACS Sustainable Chemistry & Engineering, 6 (2018) 12906-12913.
[67] J.J. Gil, O. Aguilar-Martínez, Y. Piña-Pérez, R. Pérez-Hernández, C. Santolalla-Vargas, R. Gómez, F. Tzompantzi, Efficient ZnS–ZnO/ZnAl-LDH composite for H_2 production by photocatalysis, Renewable Energy, 145 (2020) 124-132.
[68] D.P. Sahoo, S. Patnaik, K. Parida, Construction of a Z-Scheme Dictated WO_{3-X}/Ag/ZnCr LDH Synergistically Visible Light-Induced Photocatalyst towards Tetracycline Degradation and H2 Evolution, ACS Omega, 4 (2019) 14721-14741.
[69] C. Chen, H. Zeng, M. Yi, G. Xiao, S. Xu, S. Shen, B. Feng, In-situ growth of Ag_3PO_4 on calcined Zn-Al layered double hydroxides for enhanced photocatalytic degradation of tetracycline under simulated solar light irradiation and toxicity assessment, Applied Catalysis B: Environmental, 252 (2019) 47-54.
[70] G. Huang, J. Chen, D. Wang, Y. Sun, L. Jiang, Y. Yu, J. zhou, S. Ma, Y. Kang, Nb_2O_5/ZnAl–LDH composites and its calcined products for photocatalytic degradation of congo red under visible light irradiation, Materials Letters, 173 (2016) 227-230.
[71] M. Zubair, N. Jarrah, A. Khalid, M.S. Manzar, T.S. Kazeem, M.A. Al-Harthi, Starch-NiFe-layered double hydroxide composites: efficient removal of methyl orange from aqueous phase, Journal of Molecular Liquids, 249 (2018) 254-264.
[72] W. He, R. Wang, L. Zhang, J. Zhu, X. Xiang, F. Li, Enhanced photoelectrochemical water oxidation on a $BiVO_4$ photoanode modified with multi-functional layered double hydroxide nanowalls, Journal of Materials Chemistry A, 3 (2015) 17977-17982.
[73] F. Ning, M. Shao, S. Xu, Y. Fu, R. Zhang, M. Wei, D.G. Evans, X. Duan, TiO_2/graphene/NiFe-layered double hydroxide nanorod array photoanodes for efficient photoelectrochemical water splitting, Energy & Environmental Science, 9 (2016) 2633-2643.
[74] A.A. Oladipo, A.O. Ifebajo, M. Gazi, Magnetic LDH-based CoO–$NiFe_2O_4$ catalyst with enhanced performance and recyclability for efficient decolorization of azo dye via Fenton-like reactions, Applied Catalysis B: Environmental, 243 (2019) 243-252.

[75] W.-L. Jiang, X. Xia, J.-L. Han, Y.-C. Ding, M.R. Haider, A.-J. Wang, Graphene modified electro-Fenton catalytic membrane for in situ degradation of antibiotic florfenicol, Environmental science & technology, 52 (2018) 9972-9982.
[76] S.-Y. Pang, J. Jiang, J. Ma, Oxidation of sulfoxides and arsenic (III) in corrosion of nanoscale zero valent iron by oxygen: evidence against ferryl ions (Fe(IV)) as active intermediates in Fenton reaction, Environmental science & technology, 45 (2011) 307-312.
[77] H.B. Hadjltaief, P. Da Costa, P. Beaunier, M.E. Gálvez, M.B. Zina, Fe-clay-plate as a heterogeneous catalyst in photo-Fenton oxidation of phenol as probe molecule for water treatment, Applied clay science, 91 (2014) 46-54.
[78] S. Guo, G. Zhang, Y. Guo, C.Y. Jimmy, Graphene oxide–Fe_2O_3 hybrid material as highly efficient heterogeneous catalyst for degradation of organic contaminants, Carbon, 60 (2013) 437-444.
[79] H. Jin, X. Tian, Y. Nie, Z. Zhou, C. Yang, Y. Li, L. Lu, Oxygen vacancy promoted heterogeneous Fenton-like degradation of ofloxacin at pH 3.2–9.0 by Cu substituted magnetic Fe_3O_4@ FeOOH nanocomposite, Environmental science & technology, 51 (2017) 12699-12706.
[80] J. Tang, J. Wang, Iron-copper bimetallic metal-organic frameworks for efficient Fenton-like degradation of sulfamethoxazole under mild conditions, Chemosphere, 241 (2020) 125002.
[81] Y. Liu, W. Jin, Y. Zhao, G. Zhang, W. Zhang, Enhanced catalytic degradation of methylene blue by α-Fe_2O_3/graphene oxide via heterogeneous photo-Fenton reactions, Applied Catalysis B: Environmental, 206 (2017) 642-652.
[82] Q. Wang, S. Liang, G. Zhang, R. Su, C. Yang, P. Xu, P. Wang, Facile and rapid microwave-assisted preparation of Cu/Fe-AO-PAN fiber for PNP degradation in a photo-Fenton system under visible light irradiation, Separation and Purification Technology, 209 (2019) 270-278.
[83] T. Maezono, M. Tokumura, M. Sekine, Y. Kawase, Hydroxyl radical concentration profile in photo-Fenton oxidation process: generation and consumption of hydroxyl radicals during the discoloration of azo-dye Orange II, Chemosphere, 82 (2011) 1422-1430.
[84] G. Gao, Q. Zhang, Z. Hao, C.D. Vecitis, Carbon nanotube membrane stack for flow-through sequential regenerative electro-Fenton, Environmental science & technology, 49 (2015) 2375-2383.

[85] S.O. Ganiyu, T.X.H. Le, M. Bechelany, G. Esposito, E.D. Van Hullebusch, M.A. Oturan, M. Cretin, A hierarchical CoFe-layered double hydroxide modified carbon-felt cathode for heterogeneous electro-Fenton process, Journal of Materials Chemistry A, 5 (2017) 3655-3666.
[86] X. Li, S. Chen, I. Angelidaki, Y. Zhang, Bio-electro-Fenton processes for wastewater treatment: Advances and prospects, Chemical Engineering Journal, 354 (2018) 492-506.
[87] M.S. Yalfani, A. Georgi, S. Contreras, F. Medina, F.-D. Kopinke, Chlorophenol degradation using a one-pot reduction–oxidation process, Applied Catalysis B: Environmental, 104 (2011) 161-168.
[88] Z. Yang, X. Gong, B. Wang, D. Yang, T. Fu, Y. Liu, Efficient in situ generation of H_2O_2 by novel magnesium–carbon nanotube composites, RSC advances, 8 (2018) 35179-35186.
[89] Y. Chen, Z. Yang, Y. Liu, Y. Liu, Fenton-like degradation of sulfamerazine at nearly neutral pH using Fe-Cu-CNTs and Al0-CNTs for in-situ generation of H_2O_2/•OH/O_2•, Chemical Engineering Journal, (2020) 125329.
[90] Y. Liu, Q. Fan, J. Wang, Zn-Fe-CNTs catalytic in situ generation of H_2O_2 for Fenton-like degradation of sulfamethoxazole, Journal of hazardous materials, 342 (2018) 166-176.
[91] D. Wu, Y. Bai, W. Wang, H. Xia, F. Tan, S. Zhang, B. Su, X. Wang, X. Qiao, P.K. Wong, Highly pure MgO_2 nanoparticles as robust solid oxidant for enhanced Fenton-like degradation of organic contaminants, Journal of hazardous materials, 374 (2019) 319-328.
[92] Zhang, M.-h., et al., A review on Fenton process for organic wastewater treatment based on optimization perspective. Science of the total environment, 2019. **670**: p. 110-121.
[93] D. Wu, Y. Bai, W. Wang, H. Xia, F. Tan, S. Zhang, B. Su, X. Wang, X. Qiao, P.K. Wong, Highly pure MgO_2 nanoparticles as robust solid oxidant for enhanced Fenton-like degradation of organic contaminants, Journal of hazardous materials, 374 (2019) 319-328.
[94] Amina, X. Si, K. Wu, Y. Si, B. Yousaf, Synergistic effects and mechanisms of hydroxyl radical-mediated oxidative degradation of sulfamethoxazole by Fe(II)-EDTA catalyzed calcium peroxide: Implications for remediation of antibiotic-contaminated water, Chem. Eng. J. 353 (2018) 80–91.
[95] Y. Wolanov, P.V. Prikhodchenko, A.G. Medvedev, R. Pedahzur, O. Lev, Zinc dioxide nanoparticulates: a hydrogen peroxide source at moderate pH, Environ. Sci.Technol. 47 (2013) 8769–8774.

[96] A.J. Carrillo, D. Sastre, D.P. Serrano, P. Pizarro, J.M. Coronado, Revisiting the BaO_2/BaO redox cycle for solar thermochemical energy storage, Phys. Chem. Chem. Phys. 18 (2016) 8039–8048.
[97] S. Gao, M. Wang, Y. Chen, M. Tian, Y. Zhu, X. Wei, T. Jiang, An advanced electro-Fenton degradation system with triboelectric nanogenerator as electric supply and biomass-derived carbon materials as cathode catalyst, Nano Energy 45 (45) (2018) 21–27.
[98] Y. Zhu, J. Rong, T. Zhang, J. Xu, Y. Dai, F. Qiu, Facile and controlled fabrication of Cu–Al layered double hydroxide nanosheets/laccase hybrid films: a route to efficient biocatalytic removal of congo red from aqueous solutions, ACS Applied Nano Materials, 1 (2017) 284-292.
[99] R. Navik, L. Thirugnanasampanthan, H. Venkatesan, M. Kamruzzaman, F. Shafiq, Y. Cai, Synthesis and application of magnesium peroxide on cotton fabric for antibacterial properties, Cellulose, 24 (2017) 3573-3587.
[100] V. Lakshmi Prasanna, R. Vijayaraghavan, Simultaneous Fenton–photocatalytic reactions through a new single catalyst (Nano ZnO_2/Fe^{2+}) for dye degradation, The Journal of Physical Chemistry C, 121 (2017) 18557-18563.
[101] T. Kameda, T. Uchiyama, T. Yoshioka, Cu–Al layered double hydroxides intercalated with 1-naphthol-3, 8-disulfonate and dodecyl sulfate: adsorption of substituted phenols from aqueous media, New Journal of Chemistry, 39 (2015) 6315-6322.
[102] J. Xu, S. Gai, F. He, N. Niu, P. Gao, Y. Chen, P. Yang, A sandwich-type three-dimensional layered double hydroxide nanosheet array/graphene composite: fabrication and high supercapacitor performance, Journal of Materials Chemistry A, 2 (2014) 1022-1031.
[103] Z. Yang, S. Ji, W. Gao, C. Zhang, L. Ren, W.W. Tjiu, Z. Zhang, J. Pan, T. Liu, Magnetic nanomaterial derived from graphene oxide/layered double hydroxide hybrid for efficient removal of methyl orange from aqueous solution, Journal of colloid and interface science, 408 (2013) 25-32.
[104] S.L. Stupar, B.N. Grgur, M.M. Radišić, A.E. Onjia, N.D. Ivanković, A.V. Tomašević, D.Ž. Mijin, Oxidative degradation of Acid Blue 111 by electro-assisted Fenton process, Journal of Water Process Engineering, 36 (2020) 101394.
[105] N. Panda, H. Sahoo, S. Mohapatra, Decolourization of methyl orange using Fenton-like mesoporous Fe_2O_3–SiO_2 composite, Journal of hazardous materials, 185 (2011) 359-365.

[106] H. Chen, J. Motuzas, W. Martens, J.C.D. da Costa, Degradation of orange II dye under dark ambient conditions by MeSrCuO (Me= Mg and Ce) metal oxides, Separation and Purification Technology, 205 (2018) 293-301.
[107] J.P. Adjimani, P. Asare, Antioxidant and free radical scavenging activity of iron chelators, Toxicology reports, 2 (2015) 721-728.
[108] N.A. Youssef, S.A. Shaban, F.A. Ibrahim, A.S. Mahmoud, Degradation of methyl orange using Fenton catalytic reaction, Egyptian Journal of Petroleum, 25 (2016) 317-321.